General Disclaimer

One or more of the Following Statements may affect this Document

- This document has been reproduced from the best copy furnished by the organizational source. It is being released in the interest of making available as much information as possible.

- This document may contain data, which exceeds the sheet parameters. It was furnished in this condition by the organizational source and is the best copy available.

- This document may contain tone-on-tone or color graphs, charts and/or pictures, which have been reproduced in black and white.

- This document is paginated as submitted by the original source.

- Portions of this document are not fully legible due to the historical nature of some of the material. However, it is the best reproduction available from the original submission.

LOW THRUST INTERPLANETARY TRAJECTORY

OPEN LOOP ERROR ANALYSIS

Samuel Pines

Andrew H. Jazwinski

Fred I. Mann

Report No. 71 - 9
Final Report, Vol. I
Contract NAS5-11193

February 1971

ANALYTICAL MECHANICS ASSOCIATES, INC.
9430 LANHAM SEVERN ROAD
SEABROOK, MARYLAND 20801

FOREWORD

This report describes work performed under Contract NAS5-11193 for the NASA Goddard Space Flight Center. It consists of two parts. Part I presents the analytical development and Part II describes the ASTEA computer program.

ABSTRACT

This report describes the theory and computer program for the open-loop error analysis of low thrust interplanetary trajectories. The main features of the theoretical analysis and program are (i) capability to perform error analyses for rather arbitrary space trajectories; (ii) use of approximate closed form partial derivatives in the state transition matrices, resulting in significant computer time savings; (iii) capability of simulating arbitrary (as well as optional) estimators or filters. As a result, the program developed represents a very flexible tool for the evaluation of estimators and navigation systems for space missions.

TABLE OF CONTENTS

PART I

PROBLEM FORMULATION

NOMENCLATURE

Symbol	Definition
c	Exhaust speed.
c_s	Radiation pressure coefficient.
C_p	Correlation matrix of state estimation errors with p.
C_u	Correlation matrix of state estimation errors with u.
$(\hat{i}, \hat{j}, \hat{k})$	Fixed inertial coordinate system for thrust decomposition.
i_s	Unit vector to star.
I	Identity matrix.
k	Thrust magnitude.
K	Filter gain matrix.
L_o	Unit vector in radiation pressure direction.
m	Vehicle mass.
M	Matrix of measurement partials with respect to the state.
N	Matrix of measurement partials with respect to p.
p	Vector of uncertain observation parameters; pitch angle.
P	Estimation error covariance matrix; planet ephemeris position.
P_E	Heliocentric position vector of earth.
r_p	Magnitude of $R_s - P$.
r_s	Magnitude of R_s.

Symbol	Definition
r_{eq}	Equatorial radius of planet.
R	Observation noise covariance matrix.
R_p	Vehicle range vector.
R_s	Vehicle heliocentric position vector.
R_{st}	Inertial position vector of tracking station.
t	Time.
T_o	Unit vector in thrust direction.
u	Vector of uncertain dynamical parameters.
U	Covariance matrix of u.
U_p	Cross-correlation matrix of u and p.
v	Measurement noise.
W	Covariance matrix of p.
W_o	Vehicle weight.
x	State vector.
$\hat{x}$	Estimate of x.
y	Measurement vector; yaw angle.
Y	Covariance matrix of measurement residuals.
α_i	Auxiliary functions defined in text.
$\delta(\cdot)$	Perturbation or variation.
$\mathcal{E}\{\cdot\}$	Expectation (average) operator.

Symbol	Definition
λ	Magnitude of Λ.
Λ	Lagrange multiplier vector.
θ_s	Target planet - star angle.
Φ	State transition matrix.
ψ	Uncertain dynamical parameter coefficient matrix.
ψ_s	Target planet subtended angle.
μ_p	Planet mass.
μ_s	Mass of the sun.
μ_E	Mass of the earth.
σ	Standard deviation.
π	Magnitude of P .
τ	Time increment; timing error.
ρ	Range.
Ω_E	Earth angular velocity vector.

Subscripts and Superscripts

$(\dot{})$	Time derivative.
k	Index of time.
T	Vector (matrix) transpose.

1. Introduction

Part I of this report presents the analysis (equations) for a computer program which performs an open-loop error enalysis of low thrust interplanetary trajectories. Although the application presently in mind involves low thrust trajectories, our analysis and computer program are applicable to arbitrary space trajectories. The salient features of our theory are

- Arbitrary trajectories, including optimal trajectories, can be handled. For our purpose the trajectory is simply defined by a sequence of points: the actual dynamics involved need not be given.
- The use of an approximate, closed form model for partial derivatives (state transition matrix) required in the linearized error analysis obviates the time consuming integration of variational equations.
- Arbitrary estimators (filters), specified by a gain sequence, can be analyzed. The Schmidt-Kalman filter with uncertain parameters is included as an option.

Our model includes nineteen parameters associated with the dynamics (initial conditions or injection errors, propulsion system parameters, environmental parameters), and five* parameters associated with the navigation systems. Both radar tracking and on-board navigation are included. Options are available for estimating position and velocity only, or position, velocity and propulsion system parameters. Uncertainties in the parameters not estimated are taken into account.

Our model is described in Section 3. The navigation systems are presented in Section 4. The error analysis theory is given in Section 2, and is specialized to our model in Section 5. Section 6 gives the required (closed form) partial derivatives. Appendix A gives the modifications to the body of Part I of this report for the inclusion of radar station location errors.

*Currently there are eight parameters associated with the navigation systems; the additional three parameters represent station location errors. See Appendix A.

2. Error Analysis

Consider a discrete linear(ized) dynamical system with uncertain parameters, of the form

$$x_{k+1} = \Phi(k+1,k)x_k + \psi(k+1,k)u \quad , \quad k=0,\ 1,\ \ldots \ , \tag{1}$$

$$y_k = M(k)x_k + N(k)p + v_k \quad . \tag{2}$$

Equation (1) describes the dynamics; x_k is the state vector at time k, and u is the vector of uncertain dynamical parameters. Φ is the usual state transition matrix and ψ is the parameter coefficient matrix. Equation (2) describes the noisy, discrete observations taken on the state; p is the vector of uncertain observation parameters, $\{v_k\}$ is a white Gaussian noise sequence, and M, N are matrices of appropriate dimensions.

It is assumed that the statistics of x_o are known,

$$\mathcal{E}\{x_o\} = \hat{x}_o \quad , \quad \mathcal{E}\{(x_o-\hat{x}_o)(x_o-\hat{x}_o)^T\} = P_o \quad . \tag{3}*$$

The parameters u, p have the statistics

$$\begin{aligned} &\mathcal{E}\{u\} = 0 \quad , \quad \mathcal{E}\{p\} = 0 \quad , \\ &\mathcal{E}\{uu^T\} = U \quad , \quad \mathcal{E}\{pp^T\} = W \quad , \quad \mathcal{E}\{up^T\} = U_p \quad , \end{aligned} \tag{4}$$

and u, p are, respectively, uncorrelated with x_o, $\{v_k\}$. The sequence

---

* $\mathcal{E}\{\cdot\}$ is the expectation operator; superscript T denotes transposition.

$\{v_k\}$ has statistics

$$\mathcal{E}\{v_k\} = 0 \quad , \quad \mathcal{E}\{v_k\, v_k^T\} = R(k) > 0 \quad . \tag{5}$$

We assume that x_o , u and p are Gaussian, so that the sequences generated by (1) and (2) are Gaussian.

A general filter, or estimator, for the state x_k can be written as

$$\hat{x}(k+1\,|\,k) = \Phi(k+1,\ k)\ \hat{x}(k\,|\,k) \quad , \tag{6}$$

$$\hat{x}(k+1\,|\,k+1) = \hat{x}(k+1\,|\,k) + K(k+1)\left[y_{k+1} - M(k+1)\ \hat{x}(k+1\,|\,k)\right] \quad . \tag{7}$$

Eq. (6) is the prediction equation. It maps the estimate at time k , based on observations $\{\ldots, y_{k-1}, y_k\}$, to time k+1. Eq. (7) updates the estimate based on y_{k+1} ; that is, it processes observation y_{k+1} . The matrix K is the filter gain matrix. Thus $\hat{x}(i\,|\,j)$ is the estimate of x_i (the state at time i), based on the observations $\{\ldots, y_{j-1}, y_j\}$. Eqs. (6,7) are initialized with some prior estimate $\hat{x}_o$.

The open-loop error analysis of system (1,2,6,7) consists of computing the <u>state estimation error covariance matrix</u>

$$P(i\,|\,j) \triangleq \mathcal{E}\{[x_i - \hat{x}(i\,|\,j)]\,[x_i - \hat{x}(i\,|\,j)]^T\} \quad , \quad i \geq j \quad . \tag{8}$$

As we shall see, because of correlations, computation of $P(i\,|\,j)$ requires also the computation of the correlation matrices

$$C_u(i\,|\,j) \triangleq \mathcal{E}\{[x_i - \hat{x}(i\,|\,j)]\,u^T\} \quad , \tag{9}$$

$$C_p(i|j) \triangleq \mathcal{E}\{[x_i - \hat{x}(i|j)]p^T\} \quad . \tag{10}$$

For an arbitrary filter gain sequence $\{K(k)\}$, recursions for these covariance matrices are computed as

$$P(k+1|k) = \Phi(k+1,k)\, P(k|k)\, \Phi^T(k+1,k) + \Phi(k+1,k)\, C_u(k|k)\, \psi^T(k+1,k)$$

$$+ \psi(k+1,k)\, C_u^T(k|k)\, \Phi^T(k+1,k) + \psi(k+1,k)\, U\, \psi^T(k+1,k) \quad , \tag{11}$$

$$C_u(k+1|k) = \Phi(k+1,k)\, C_u(k|k) + \psi(k+1,k)\, U \quad , \tag{12}$$

$$C_p(k+1|k) = \Phi(k+1,k)\, C_p(k|k) + \psi(k+1,k)\, U_p \quad , \tag{13}$$

$$P(k+1|k+1) = [I - K(k+1)\, M(k+1)]\, P(k+1|k)\, [I - K(k+1)\, M(k+1)]^T$$

$$- [I - K(k+1)\, M(k+1)]\, C_p(k+1|k)\, N^T(k+1)\, K^T(k+1)$$

$$- K(k+1)\, N(k+1)\, C_p^T(k+1|k)\, [I - K(k+1)\, M(k+1)]^T$$

$$+ K(k+1)\, N(k+1)\, W\, N^T(k+1)\, K^T(k+1) + K(k+1)\, R(k+1)\, K^T(k+1) \quad , \tag{14}$$

$$C_u(k+1|k+1) = C_u(k+1|k) - K(k+1)\, [M(k+1)\, C_u(k+1|k) + N(k+1)\, U_p^T] \quad , \tag{15}$$

$$C_p(k+1|k+1) = C_p(k+1|k) - K(k+1)\, [M(k+1)\, C_p(k+1|k) + N(k+1)\, W] \quad . \tag{16}$$

Equations (11-16) are initialized with $P(0|0) = P_o$, $C_u(0|0) = 0$, $C_p(0|0) = 0$. Note that these equations are coupled.

The optimal (minimum variance) filter for the state x_k, which takes into account the fact that the parameters u and p are uncertain, but does not estimate them, is the Schmidt-Kalman filter with uncertain parameters. This filter is developed and discussed in [2]. Its gain is given by

$$K(k+1) = [P(k+1|k)\, M^T(k+1) + C_p(k+1|k)\, N^T(k+1)]\, Y^{-1}(k+1) \quad , \tag{17}$$

where

$$Y(k+1) = M(k+1)\, P(k+1|k)\, M^T(k+1) + M(k+1)\, C_p(k+1|k)\, N^T(k+1)$$

$$+ N(k+1)\, C_p^T(k+1|k)\, M^T(k+1) + N(k+1)\, W\, N^T(k+1) + R(k+1) \quad . \tag{18}$$

For this filter, Eqs. (11-13, 15, 16) remain as given, while (14) simplifies to

$$P(k+1|k+1) = P(k+1|k) - K(k+1)\, [M(k+1)\, P(k+1|k) + N(k+1)\, C_p^T(k+1|k)] \quad . \tag{14}_{sk}$$

Recapitulating, solution of Eqs. (11-16) produces the error analysis. That is, $P(\ell|k)$, $\ell \geq k$, tells us how well the state can be estimated <u>given</u> a certain navigation scheme; that is, given $\{y_1, \ldots, y_k\}$ and given the filter to be used. The i^{th} diagonal element of $P(\ell|k)$ is the variance of the error in the estimate of the i^{th} component of the state vector x_ℓ, having processed the observations $\{y_1, \ldots, y_k\}$. Now the Schmidt-Kalman filter with gain (17) is unbiased, so that for that filter the estimation error is zero-mean. Eqs. (11-13) are prediction equations, while Eqs. (14-16) update the error covariances based on each new observation.

To illustrate recursions (11-16), suppose the problem starts at time 0, and observations are available at times 1, 2, ... Starting with $P(0|0)$, $C_u(0|0)$, $C_p(0|0)$, as specified below (16), Eqs. (11-13) are used to compute

$P(1|0)$, $C_u(1|0)$ and $C_p(1|0)$. These are error covariances at time 1 given no observations. Now Eqs. (14-16) are used to compute $P(1|1)$, $C_u(1|1)$, $C_p(1|1)$. These are the error covariances at time 1 given y_1. This procedure is continued until all observations have been processed. Eqs. (11-13) can then be used to predict the error variances beyond times where observations are available.

3. Environment and Propulsion System Models

Environmental and propulsion system errors and error sensitivity models (partial derivatives) are based on an extension of the theory developed in [1]. In essence, it is assumed that over short time intervals (days) :

(a) central body (solar) gravitational field is uniform,

(b) target planet gravitational field is uniform,

(c) thrust time rate of change and mass flow rate are constant, and

(d) solar radiation pressure field is uniform.

Under these assumptions, the motion of the space vehicle in heliocentric cartesian coordinates is described by

$$\ddot{R}_s(t) = -\mu_s \frac{R_{so}}{r_{so}^3} - \mu_p \left[\frac{R_{so} - P}{r_p^3} + \frac{P}{\pi^3} \right]$$

$$+ \frac{k}{m} \left[T_o + \dot{T}_o (t - t_o) \right] + \frac{c_s}{r_{so}^2} L_o \quad , \tag{19}$$

$$\dot{m} = -\frac{k}{c} \quad . \tag{20}$$

The sketch below

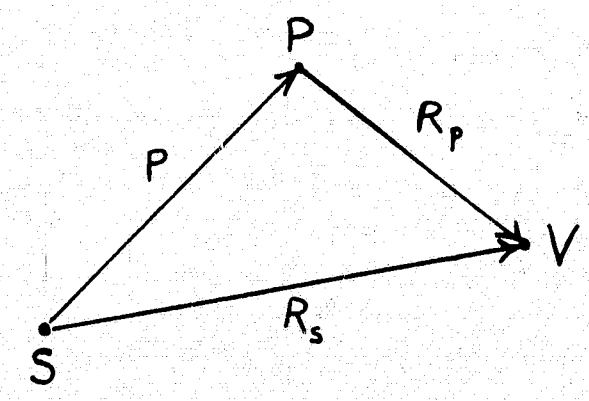

defines R_s and P, which are, respectively, the vehicle position vector and the planet position vector. Also,

$$r_{so} = |R_{so}| , \quad \pi = |P| , \quad r_p = |R_p| = |R_{so} - P| , \tag{21}$$

where R_{so} is a fixed (constant) value of R_s. R_{so} and P are assumed constant in each time interval. k is the thrust magnitude, c is the exhaust speed, T_o the unit vector in the thrust direction ($|T_o| = 1$), and $\dot{T}_o = dT_o/dt$; all assumed constant in each time interval. c_s is the radiation pressure coefficient and L_o the unit vector in the radiation pressure direction ($|L_o| = 1$), both assumed constant in each time interval.

We can immediately integrate (20) from t_{i-1} to t_i to get the mass $m(t_i)$, or equivalently, the weight $W(t_i)$

$$W(t_i) = W_o + \dot{W}_o \tau \tag{22}$$

where

$$\tau = t_i - t_{i-1} .$$

Then (19) is integrated to produce

$$R_s(t_i) = R_{so} + \dot{R}_{so}\tau$$

$$- \left[\mu_s \frac{R_{so}}{r_{so}^3} + \mu_p \left(\frac{R_{so} - P}{r_p^3} + \frac{P}{\pi^3} \right) - \frac{c_s}{r_{so}^2} L_o \right] \frac{\tau^2}{2}$$

$$+ c T_o \left[\tau + \frac{W_o + \dot{W}_o \tau}{\dot{W}_o} \ell n \left(\frac{W_o}{W_o + \dot{W}_o \tau}\right)\right]$$

$$- c \dot{T}_o \left\{\frac{\tau^2}{2} + \frac{W_o}{\dot{W}_o}\left[\tau + \frac{W_o + \dot{W}_o \tau}{\dot{W}_o} \ell n \left(\frac{W_o}{W_o + \dot{W}_o \tau}\right)\right]\right\}, \qquad (23)$$

$$\dot{R}_s(t_i) = \dot{R}_{so} - \left[\mu_s \frac{R_{so}}{r_{so}^3} + \mu_p \left(\frac{R_{so} - P}{r_p^3} + \frac{P}{\pi^3}\right) - \frac{c_s}{r_{so}^2} L_o\right] \tau$$

$$+ c T_o \ell n \left(\frac{W_o}{W_o + \dot{W}_o \tau}\right) - c \dot{T}_o \left[\tau + \frac{W_o}{\dot{W}_o} \ell n \left(\frac{W_o}{W_o + \dot{W}_o \tau}\right)\right]. \qquad (24)$$

The thrust direction will be specified in terms of fixed inertial coordinates defined by the vehicle's initial position and velocity vectors, R_{oo} and $\dot{R}_{oo}$, respectively. That coordinate system is defined by the unit vectors

$$\hat{j} = \frac{R_{oo}}{r_{oo}} \quad ,$$

$$\hat{k} = \frac{R_{oo} \times \dot{R}_{oo}}{|R_{oo} \times \dot{R}_{oo}|} \quad , \qquad (25)$$

$$\hat{i} = \hat{k} \times \hat{j} \quad ,$$

and is shown in the sketch

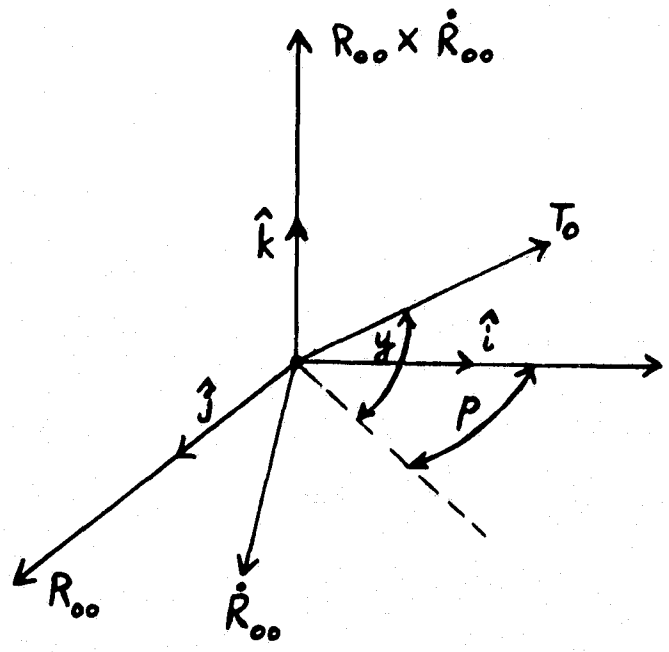

In this coordinate system, the pitch angle p and yaw angle y are defined as indicated. Then the thrust direction is given by

$$T_o = (\cos y \cos p)\,\hat{i} + (\cos y \sin p)\,\hat{j} + (\sin y)\,\hat{k} \quad , \tag{26}$$

and

$$\dot{T}_o = -\,(\dot{y} \sin y \cos p + \dot{p} \cos y \sin p)\,\hat{i} + (\dot{p} \cos y \cos p - \dot{y} \sin y \sin p)\,\hat{j}$$

$$+ (\dot{y} \cos y)\,\hat{k} \quad , \tag{27}$$

where $\dot{p}$ and $\dot{y}$ are pitch rate and yaw rate, respectively. Substitution of (26) and (27) into (23) and (24) yields the desired model.

Now it is not our intent to approximate the trajectory dynamics by Eqs. (19), (20)

for the whole duration of the mission. Rather, we fit Eqs. (22)-(24) to short arcs of a precision trajectory. More precisely, we fit partial derivatives (sensitivities) of $R_s(t_i)$, $\dot{R}_s(t_i)$ and $W(t_i)$ with respect to the various propulsion system and environmental parameters, as well as initial conditions, appearing in (22)-(24), (26), (27). We will identify these parameters below. The approximate partial derivatives thus obtained are used to propagate error statistics over short arcs (from t_{i-1} to t_i), based on the linear theory described in Sections 2 and 5. The partial derivatives are given in Section 6.

The fit is accomplished in the following way. At a sequence of times $\{t_k\}$, the following data from the precision trajectory are used:

$$t_k\ ,\ R_k\ ,\ \dot{R}_k\ ,\ T_k\ (\Lambda_k)\ ,\ \dot{T}_k\ (\dot{\Lambda}_k)\ ,\ W_k\ ,\ \dot{W}_k\ ,$$

$$c_{s_k}\ ,\ L_k\ ,\ P_k\ . \tag{28}$$

R_k is the position vector, $\dot{R}_k$ the velocity vector, T_k the unit thrust vector, $\dot{T}_k$ its rate, W_k the weight, $\dot{W}_k$ the weight rate, c_{s_k} the solar pressure coefficient, L_k the unit solar pressure vector, and P_k the target planet ephemeris position vector. In case the precision trajectory is an optimal trajectory, then instead of T_k and $\dot{T}_k$, Λ_k and $\dot{\Lambda}_k$ are used. These are, respectively, the Lagrange multiplier vector and its rate. In addition to these data, the mass constants μ_s and μ_p, and jet exhaust speed c, for the precision trajectory are used.

Then the constants in our model [in Eqs. (22)-(24), (26), (27)] are computed as follows:

$$\tau = t_i - t_{i-1}\ ,$$

$$R_{so} = \tfrac{1}{2}\,(R_i + R_{i-1})\ ,\quad r_{so} = |R_{so}|\ ,$$

$$\dot{R}_{so} = \dot{R}_{i-1}\ ,$$

$$P = \tfrac{1}{2}\,(P_i + P_{i-1})\ ,\quad \pi = |P|\ ,$$

$$R_p = R_{so} - P\ ,\quad r_p = |R_p|\ ,$$

$$W_o = W_{i-1}\ ,$$

$$\dot{W}_o = \tfrac{1}{2}\,(\dot{W}_i + \dot{W}_{i-1})\ , \qquad (29)$$

$$T_o = T_{i-1} \qquad\qquad T_o = \Lambda_{i-1}/\lambda_{i-1}\ ,\ \lambda_{i-1} = |\Lambda_{i-1}|\ ,$$

or

$$\dot{T}_o = \dot{T}_{i-1} \qquad\qquad \dot{T}_o = -\Lambda_{i-1} \times (\Lambda_{i-1} \times \dot{\Lambda}_{i-1})/\lambda_{i-1}^3\ ,$$

$$L_o = \tfrac{1}{2}\,(L_i + L_{i-1})\ ,$$

$$c_s = \tfrac{1}{2}\,(c_{s_i} + c_{s_{i-1}})\ .$$

The fixed inertial coordinate system for thrust representation (25) is established using the first trajectory point (28). Then the pitch, yaw, pitch rate and yaw rate are computed

$$p = \tan^{-1}\left[\frac{\hat{j}^T T_o}{\hat{i}^T T_o}\right]\ ,$$

$$y = \sin^{-1}\left[\hat{k}^T T_o\right] ,$$

$$\dot{y} = \frac{\hat{k}^T \dot{T}_o}{\cos y} \quad , \tag{30}$$

$$\dot{p} = \frac{\cos p}{\cos y}\ \hat{j}^T \dot{T}_o - \frac{\sin p}{\cos y}\ \hat{i}^T \dot{T}_o \quad .$$

It is observed from Eqs. (22)-(24), (26), (27) that our model includes the initial conditions

$$R_s(t_{i-1}) \ , \ \dot{R}_s(t_{i-1}) \ , \tag{31}$$

(denoted here by R_{so} and $\dot{R}_{so}$) , the propulsion system parameters

$$W_o, \ \dot{W}_o, \ c, \ p, \ y, \ \dot{p}, \ \dot{y} \ , \tag{32}$$

and the environmental parameters

$$\mu_s \ , \ \mu_p \ , \ P \ , \ c_s \ . \tag{33}$$

That is, $R_s(t_i)$ and $\dot{R}_s(t_i)$ are functions of the nineteen scalar parameters given in (31)-(33).

Using the linear estimation theory described in Section 2, our model enables an error analysis where errors in (31) represent injection errors; errors in W_o, $\dot{W}_o$ and c, model errors in thrust magnitude, errors in p, y, $\dot{p}$ and $\dot{y}$,

model errors in thrust orientation; errors in μ_s and μ_p, model gravitational errors; errors in P, model ephemeris errors; and errors in c_s, model errors in the solar radiation pressure. To put our model in the linear form of Eq. (1), we expand (22)-(24), (26), (27) to first order around the values given in (29), (30). We thus obtain the perturbations, or variations, or errors

$$\delta R_s(t_i) , \quad \delta \dot{R}_s(t_i) , \quad \delta W(t_i)$$

as linear functions of perturbations of the variables listed in (31)-(33). This is described in detail in Section 5. The partial derivatives in this expansion are given in Section 6.

4. Navigation Systems

We consider two navigation modes; earth ground-based radar tracking and on-board angle measurements. These are described in the next two subsections. The partial derivatives required in the linear error analysis are given in Section 6.

4.1 Ground-Based Tracking

Ground-based tracking will consist of range rate ($\dot{\rho}$) observations from earth tracking stations. Referring to the sketch below, range is given by

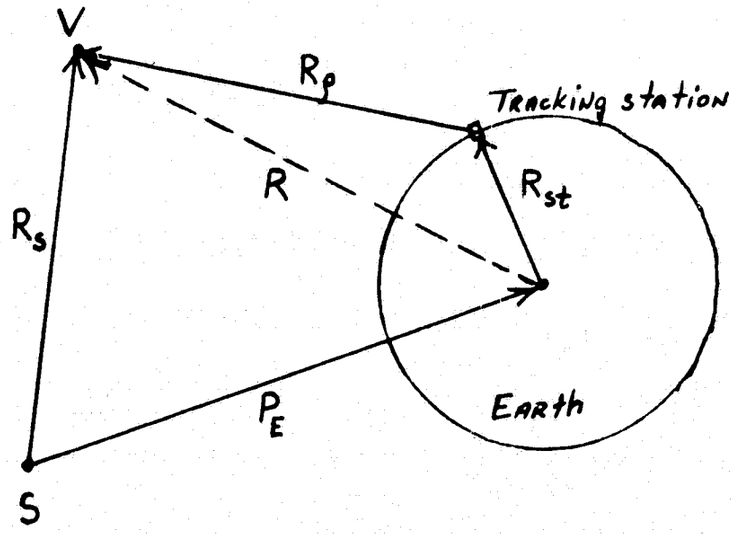

$$\rho = |R_\rho|$$

and range rate by

$$\dot{\rho} = \frac{R_\rho^T \dot{R}_\rho}{|R_\rho|} \quad , \tag{34}$$

where

$$R_{\rho} = R_s - P_E - R_{st} . \tag{35}$$

We assume that the range rate observation is contaminated by zero-mean, white Gaussian noise $v_{\dot{\rho}}$, so that we observe

$$y_{\dot{\rho}} = \dot{\rho} + v_{\dot{\rho}} . \tag{36}$$

Furthermore, we suppose that the range rate observation has a zero-mean timing error $\tau_{\dot{\rho}}$, and that the partial of $\dot{\rho}$ with respect to the timing error is

$$\frac{\partial \dot{\rho}}{\partial \tau_{\dot{\rho}}} \triangleq \frac{d\dot{\rho}}{dt} .$$

Then the linearized range rate observation becomes

$$\delta y_{\dot{\rho}} = \left(\frac{\partial \dot{\rho}}{\partial R_s}\right) \delta R_s + \left(\frac{\partial \dot{\rho}}{\partial \dot{R}_s}\right) \delta \dot{R}_s + \frac{d\dot{\rho}}{dt} \tau_{\dot{\rho}} + v_{\dot{\rho}} . \tag{37}$$

To summarize, errors in the range rate observations consist of timing errors (an uncertain parameter) and a random error component.*

4.2 On-Board Navigation

On-board observations will consist of the target planet-star angle θ_s, and the target planet subtended angle ψ_s.

*Station location errors have been added. See Appendix A.

Referring to the sketch below, θ_s is given by

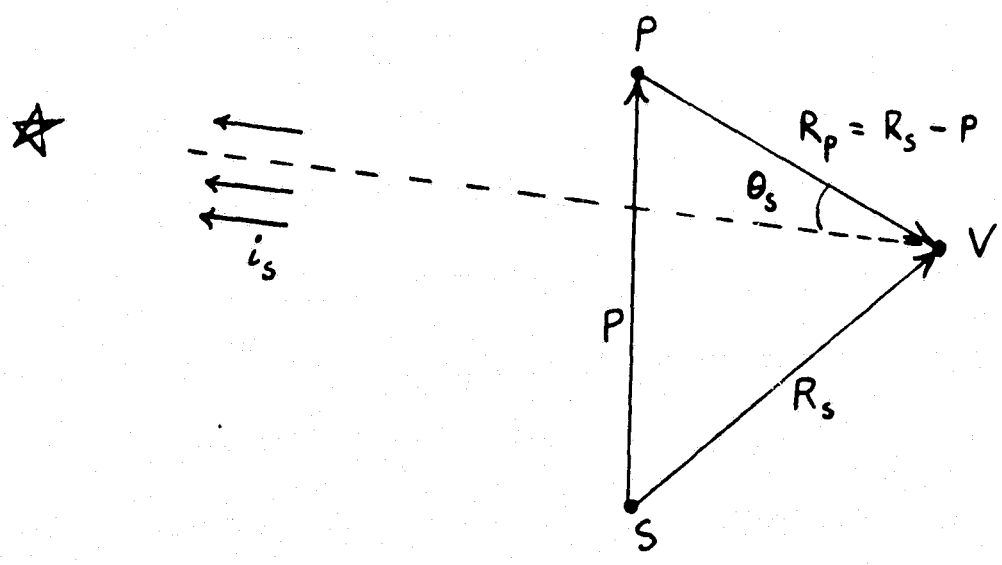

$$\theta_s = \cos^{-1}\left[\frac{(P-R_s)^T i_s}{|P-R_s|}\right] , \tag{38}$$

where i_s is the unit vector in the star direction. We suppose that there is a zero-mean error in P (ephemeris error), a zero-mean timing error τ_{θ_s} (error in the on-board clock), and that the observation is contaminated by zero-mean white Gaussian noise. Thus the linearized planet-star angle observation is

$$\delta y_{\theta_s} = \left(\frac{\partial \theta_s}{\partial R_s}\right) \delta R_s + \left(\frac{\partial \theta_s}{\partial P}\right) \delta P + \frac{d\theta_s}{dt} \tau_{\theta_s} + v_{\theta_s} . \tag{39}$$

With the aid of the following sketch, the planet subtended angle ψ_s is

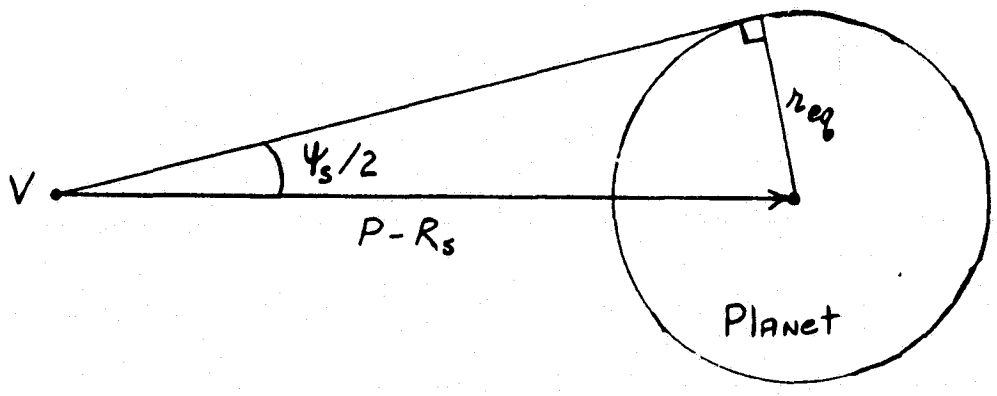

given by

$$\psi_s = 2 \sin^{-1} \left(\frac{r_{eq}}{|P - R_s|} \right) . \tag{40}$$

Again assuming ephemeris errors δP, timing error τ_{ψ_s}, and a random Gaussian noise component, the linearized subtended angle observation becomes

$$\delta y_{\psi_s} = \left(\frac{\partial \psi_s}{\partial R_s} \right) \delta R_s + \left(\frac{\partial \psi_s}{\partial P} \right) \delta P + \frac{d\psi_s}{dt} \tau_{\psi_s} + v_{\psi_s} . \tag{41}$$

5. Theory Specialized*

In specializing the error analysis of Section 2 to the low thrust interplanetary trajectory error models developed in Sections 3 and 4, we consider two optional modes. In Mode 1 the state vector (being estimated) is defined to be

$$x^T \triangleq \left[\delta R_s^T \; \delta \dot{R}_s^T \; \delta W_o \; \delta \dot{W}_o \; \delta c \; \delta p \; \delta y \; \delta \dot{p} \; \delta \dot{y} \right] \; ; \qquad (42)_1$$

that is, x is a 13×1 vector. The vector u of uncertain dynamical parameters is the 6×1 vector

$$u^T \triangleq \left[\delta \mu_s \; \delta \mu_p \; \delta P^T \; \delta c_s \right] , \qquad (43)_1$$

and the vector p of uncertain observation parameters is the 5×1 vector

$$p^T \triangleq \left[\tau_{\dot{\rho}} \; \delta P^T \; \tau_a \right] , \qquad (44)$$

where τ_a is the on-board clock error (either τ_{θ_s} or τ_{ψ_s}). In Mode 2 the state vector x is taken as the 6×1 vector

$$x^T \triangleq \left[\delta R_s^T \; \delta \dot{R}_s^T \right] , \qquad (42)_2$$

while the vector u of uncertain dynamical parameters is taken as the 13×1 vector

$$u^T \triangleq \left[\delta W_o \; \delta \dot{W}_o \; \delta c \; \delta p \; \delta y \; \delta \dot{p} \; \delta \dot{y} \; \delta \mu_s \; \delta \mu_p \; \delta P^T \; \delta c_s \right] . \qquad (43)_2$$

*Modifications to this section resulting from addition of station location errors are given in Appendix A.

The vector p of uncertain observation parameters is the same, that is, as given in (44). $\delta(\cdot)$ denotes a small perturbation, or variation, or error.

5.1 Mode 1

In this mode, the state transition matrix Φ of Section 2 is clearly the 13x13 matrix of partial derivatives

$$\Phi(i, i-1) = \left[\begin{array}{ccccccccc}
\underset{(3x3)}{\frac{\partial R_s(t_i)}{\partial R_s(t_{i-1})}}, & \underset{(3x3)}{\frac{\partial R_s(t_i)}{\partial \dot{R}_s(t_{i-1})}}, & \underset{(3x1)}{\frac{\partial R_s(t_i)}{\partial W_o}}, & \underset{(3x1)}{\frac{\partial R_s(t_i)}{\partial \dot{W}_o}}, & \underset{(3x1)}{\frac{\partial R_s(t_i)}{\partial c}}, & \underset{(3x1)}{\frac{\partial R_s(t_i)}{\partial p}}, & \underset{(3x1)}{\frac{\partial R_s(t_i)}{\partial y}}, & \underset{(3x1)}{\frac{\partial R_s(t_i)}{\partial \dot{p}}}, & \underset{(3x1)}{\frac{\partial R_s(t_i)}{\partial \dot{y}}} \\
\underset{(3x3)}{\frac{\partial \dot{R}_s(t_i)}{\partial R_s(t_{i-1})}}, & \underset{(3x3)}{\frac{\partial \dot{R}_s(t_i)}{\partial \dot{R}_s(t_{i-1})}}, & \underset{(3x1)}{\frac{\partial \dot{R}_s(t_i)}{\partial W_o}}, & \underset{(3x1)}{\frac{\partial \dot{R}_s(t_i)}{\partial \dot{W}_o}}, & \underset{(3x1)}{\frac{\partial \dot{R}_s(t_i)}{\partial c}}, & \underset{(3x1)}{\frac{\partial \dot{R}_s(t_i)}{\partial p}}, & \underset{(3x1)}{\frac{\partial \dot{R}_s(t_i)}{\partial y}}, & \underset{(3x1)}{\frac{\partial \dot{R}_s(t_i)}{\partial \dot{p}}}, & \underset{(3x1)}{\frac{\partial \dot{R}_s(t_i)}{\partial \dot{y}}} \\
\underset{(1x3)}{0}, & \underset{(1x3)}{0}, & 1, & \tau, & 0, & 0, & 0, & 0, & 0 \\
\hline
\multicolumn{2}{c|}{\underset{(6x7)}{0}} & 1, & 0, & 0, & 0, & 0, & 0 \\
 & & 0, & 1, & 0, & 0, & 0, & 0 \\
 & & 0, & 0, & 1, & 0, & \tau, & 0 \\
 & & 0, & 0, & 0, & 1, & 0, & \tau \\
 & & 0, & 0, & 0, & 0, & 1, & 0 \\
 & & 0, & 0, & 0, & 0, & 0, & 1
\end{array}\right], \quad (45)$$

and the matrix ψ is the 13x6 matrix

$$\psi(i,\ i-1) = \begin{bmatrix} \underset{(3x1)}{\frac{\partial R_s(t_i)}{\partial \mu_s}} , \underset{(3x1)}{\frac{\partial R_s(t_i)}{\partial \mu_p}} , \underset{(3x3)}{\frac{\partial R_s(t_i)}{\partial P}} , \underset{(3x1)}{\frac{\partial R_s(t_i)}{\partial c_s}} \\ \\ \underset{(3x1)}{\frac{\partial \dot{R}_s(t_i)}{\partial \mu_s}} , \underset{(3x1)}{\frac{\partial \dot{R}_s(t_i)}{\partial \mu_p}} , \underset{(3x3)}{\frac{\partial \dot{R}_s(t_i)}{\partial P}} , \underset{(3x1)}{\frac{\partial \dot{R}_s(t_i)}{\partial c_s}} \\ \\ \text{- - - - - - - - - - - - - - - - - - - -} \\ \\ \underset{(7x6)}{0} \end{bmatrix} . \tag{46}$$

The partial derivative matrices (vectors) appearing in (45), (46) are obtained by differentiating (23), (24), and are given in Section 6. The (constant) covariance matrix U of Eq. (4), assuming no correlations, is the 6x6 diagonal matrix

$$\text{diag } U = \left(\sigma^2_{\mu_s} , \sigma^2_{\mu_p} , \sigma^2_{P_1} , \sigma^2_{P_2} , \sigma^2_{P_3} , \sigma^2_{c_s} \right) , \tag{47}$$

where σ^2_i are the variances of the uncertain dynamical parameters u_i. P_i is the i^{th} component of the target planet position vector P. The (constant) covariance matrix U_p of Eq. (4) is 6x5 ,

$$U_p = \begin{bmatrix} 0 & 0 & 0 & 0 & 0 \\ 0 & 0 & 0 & 0 & 0 \\ 0 & \sigma^2_{P_1} & 0 & 0 & 0 \\ 0 & 0 & \sigma^2_{P_2} & 0 & 0 \\ 0 & 0 & 0 & \sigma^2_{P_3} & 0 \\ 0 & 0 & 0 & 0 & 0 \end{bmatrix} . \tag{48}$$

The initial state estimation error covariance matrix is 13x13, assumed diagonal,

$$\text{diag } P_o = \Big(\sigma^2_{R_{s_1}}, \sigma^2_{R_{s_2}}, \sigma^2_{R_{s_3}}, \sigma^2_{\dot{R}_{s_1}}, \sigma^2_{\dot{R}_{s_2}}, \sigma^2_{\dot{R}_{s_3}}, \sigma^2_{W_o}, \sigma^2_{\dot{W}_o}, \sigma^2_c, \sigma^2_p, \sigma^2_y, \sigma^2_{\dot{p}}, \sigma^2_{\dot{y}} \Big) . \tag{49}$$

where R_{s_i}, $\dot{R}_{s_i}$ are, respectively, the i^{th} components of the vehicle position and velocity vectors. Clearly the matrix $P(i|j)$ is 13x13, $C_u(i|j)$ is 13x6, and $C_p(i|j)$ is 13x5.

For ground-based tracking of Section 4.1, the range rate observation y_i and noise v_i are scalar, the matrix M is 1x13,

$$M(i) = \Big[\underset{(1x3)}{\frac{\partial \dot{\rho}}{\partial R_s}}, \underset{(1x3)}{\frac{\partial \dot{\rho}}{\partial \dot{R}_s}}, 0, 0, 0, 0, 0, 0, 0 \Big] , \tag{50}$$

and the matrix N is 1x5,

$$N(i) = \left[\frac{d\dot{\rho}}{dt} , \ 0, \ 0, \ 0, \ 0 \right] . \tag{51}$$

The partials in (50, (51) are given in Section 6. The (constant) covariance matrix W of Eq. (4), assuming no correlations, is the 5x5 diagonal matrix

$$\text{diag } W = \left(\sigma^2_{\tau_{\dot{\rho}}} , \ \sigma^2_{P_1} , \ \sigma^2_{P_2} , \ \sigma^2_{P_3} , \ \sigma^2_{\tau_a} \right) , \tag{52}$$

where σ^2_i are the variances of the uncertain observation parameters p_i .
The noise covariance matrix R of Eq. (5) is scalar,

$$R(i) = \sigma^2_{v_{\dot{\rho}}} . \tag{53}$$

For on-board navigation of Section 4.2, the observation y_i is a 2x1 vector consisting of the planet-star angle and the planet subtended angle; that is

$$y_i = \begin{bmatrix} \delta y_{\theta_s} \\ \delta y_{\psi_s} \end{bmatrix} = \begin{bmatrix} \frac{\partial \theta_s}{\partial R_s} \\ \frac{\partial \psi_s}{\partial R_s} \end{bmatrix} \delta R_s + \begin{bmatrix} \frac{\partial \theta_s}{\partial P} \\ \frac{\partial \psi_s}{\partial P} \end{bmatrix} \delta P + \begin{bmatrix} \frac{d\theta_s}{dt} \\ \frac{d\psi_s}{dt} \end{bmatrix} \tau_a + \begin{bmatrix} v_{\theta_s} \\ v_{\psi_s} \end{bmatrix} . \tag{54}$$

Therefore, the matrix M is 2x13,

$$M(i) = \left[\begin{array}{c|c} \begin{matrix} (1x3) \\ \frac{\partial \theta_s}{\partial R_s} \\ (1x3) \\ \frac{\partial \psi_s}{\partial R_s} \end{matrix} & \begin{matrix} (2x10) \\ 0 \end{matrix} \end{array} \right] , \tag{55}$$

and the matrix N is 2x5 ,

$$N(i) = \begin{bmatrix} & \overset{(1x3)}{} & \\ 0\,, & \dfrac{\partial\theta_s}{\partial P} & , \dfrac{d\theta_s}{dt} \\ & \overset{(1x3)}{} & \\ 0\,, & \dfrac{\partial\psi_s}{\partial P} & , \dfrac{d\psi_s}{dt} \end{bmatrix} . \qquad (56)$$

The covariance matrix W is as given in (52), while the noise covariance matrix R is 2x2 diagonal,

$$R(i) = \begin{bmatrix} \sigma^2_{v_{\theta_s}} & 0 \\ 0 & \sigma^2_{v_{\psi_s}} \end{bmatrix} . \qquad (57)$$

5.2 Mode 2

In Mode 2, the state transition matrix Φ is the 6x6 matrix of partial derivatives

$$\Phi(i,\, i-1) = \begin{bmatrix} \overset{(3x3)}{\dfrac{\partial R_s(t_i)}{\partial R_s(t_{i-1})}} & , \overset{(3x3)}{\dfrac{\partial R_s(t_i)}{\partial \dot{R}_s(t_{i-1})}} \\ \overset{(3x3)}{\dfrac{\partial \dot{R}_s(t_i)}{\partial R_s(t_{i-1})}} & \overset{(3x3)}{\dfrac{\partial \dot{R}_s(t_i)}{\partial \dot{R}_s(t_{i-1})}} \end{bmatrix} , \qquad (58)$$

and the matrix ψ is the 6x13 matrix

$$\psi(i,\ i-1) =$$

$$\begin{bmatrix} \frac{\partial R_s(t_i)}{\partial W_o}_{(3x1)}, & \frac{\partial R_s(t_i)}{\partial \dot{W}_o}_{(3x1)}, & \frac{\partial R_s(t_i)}{\partial c}_{(3x1)}, & \frac{\partial R_s(t_i)}{\partial p}_{(3x1)}, & \frac{\partial R_s(t_i)}{\partial y}_{(3x1)}, & \frac{\partial R_s(t_i)}{\partial \dot{p}}_{(3x1)}, & \frac{\partial R_s(t_i)}{\partial \dot{y}}_{(3x1)}, & \frac{\partial R_s(t_i)}{\partial \mu_s}_{(3x1)}, & \frac{\partial R_s(t_i)}{\partial \mu_p}_{(3x1)}, & \frac{\partial R_s(t_i)}{\partial P}_{(3x3)}, & \frac{\partial R_s(t_i)}{\partial c_s}_{(3x1)} \\ \frac{\partial \dot{R}_s(t_i)}{\partial W_o}_{(3x1)}, & \frac{\partial \dot{R}_s(t_i)}{\partial \dot{W}_o}_{(3x1)}, & \frac{\partial \dot{R}_s(t_i)}{\partial c}_{(3x1)}, & \frac{\partial \dot{R}_s(t_i)}{\partial p}_{(3x1)}, & \frac{\partial \dot{R}_s(t_i)}{\partial y}_{(3x1)}, & \frac{\partial \dot{R}_s(t_i)}{\partial \dot{p}}_{(3x1)}, & \frac{\partial \dot{R}_s(t_i)}{\partial \dot{y}}_{(3x1)}, & \frac{\partial \dot{R}_s(t_i)}{\partial \mu_s}_{(3x1)}, & \frac{\partial \dot{R}_s(t_i)}{\partial \mu_p}_{(3x1)}, & \frac{\partial \dot{R}_s(t_i)}{\partial P}_{(3x3)}, & \frac{\partial \dot{R}_s(t_i)}{\partial c_s}_{(3x1)} \end{bmatrix} . \quad (59)$$

The covariance matrix U is the 13x13 diagonal matrix

$$\text{diag } U = \Big(\sigma^2_{W_o}\ ,\ \sigma^2_{\dot{W}_o}\ ,\ \sigma^2_c\ ,\ \sigma^2_p\ ,\ \sigma^2_y\ ,\ \sigma^2_{\dot{p}}\ ,\ \sigma^2_{\dot{y}}\ ,\ \sigma^2_{\mu_s}\ ,\ \sigma^2_{\mu_p}\ ,$$

$$\sigma^2_{P_1}\ ,\ \sigma^2_{P_2}\ ,\ \sigma^2_{P_3}\ ,\ \sigma^2_{c_s}\ \Big) \ . \quad (60)$$

U_p is 13x5 with all elements zero except

$$\big(U_p\big)_{10,2} = \sigma^2_{P_1}\ ,\ \big(U_p\big)_{11,3} = \sigma^2_{P_2}\ ,\ \big(U_p\big)_{12,4} = \sigma^2_{P_3} \ . \quad (61)$$

The initial state estimation error covariance matrix is 6x6,

$$\text{diag } P_o = \Big(\sigma^2_{R_{s_1}}\ ,\ \sigma^2_{R_{s_2}}\ ,\ \sigma^2_{R_{s_3}}\ ,\ \sigma^2_{\dot{R}_{s_1}}\ ,\ \sigma^2_{\dot{R}_{s_2}}\ ,\ \sigma^2_{\dot{R}_{s_3}}\ \Big) \ . \quad (62)$$

The matrix $P(i|j)$ is 6x6, $C_u(i|j)$ is 6x13, and $C_p(i|j)$ is 6x5.

For ground-based tracking of Section 4.1, the matrix M is 1x6, consisting of the first six elements of M in (50). The matrix N is identical to that in Mode 1, that is, as given in (51). Also, W is 5x5, given in (52), and R is scalar, given in (53).

For on-board navigation of Section 4.2, the matrix M is 2x6, consisting of the first six columns of M in (55). N is 2x5, as given in (56). W is 5x5, given in (52), and R is 2x2, as given in (57).

6. Partial Derivatives

Define the auxiliary variables

$$\alpha_1 = \frac{\dot{W}_o}{W_o + \dot{W}_o \tau} \quad ,$$

$$\alpha_3 = \cos p \quad ,$$

$$\alpha_4 = \sin p \quad ,$$

$$\alpha_5 = \cos y \quad ,$$

$$\alpha_6 = \sin y \quad ,$$

$$\alpha_7 = \alpha_3 \, \alpha_5 \quad ,$$

$$\alpha_8 = \alpha_3 \, \alpha_6 \quad ,$$

$$\alpha_9 = \alpha_4 \, \alpha_5 \quad ,$$

$$\alpha_{10} = \alpha_4 \, \alpha_6 \quad ,$$

$$\alpha_{18} = \ell n \left(\frac{W_o}{W_o + \dot{W}_o \tau} \right) \quad ,$$

$$\alpha_{19} = \tau + \frac{\alpha_{18}}{\alpha_1} \quad ,$$

$$\alpha_{20} = \tau + \frac{W_o}{\dot{W}_o} \, \alpha_{18} \quad , \tag{63}$$

$$\alpha_{21} = \frac{\tau^2}{2} + \frac{W_o}{\dot{W}_o} \, \alpha_{19} \quad .$$

Then the partial derivatives appearing in the matrices Φ and ψ of Section 5, obtained by differentiating (23), (24), are given as

$$\frac{\partial R_s(t_i)}{\partial R_s(t_{i-1})} = \left[1 - \left(\frac{\mu_s}{3 r_{so}^3} + \frac{\mu_p}{3 r_p^3}\right) \frac{\tau^2}{2}\right] I + \frac{3\mu_s \tau^2}{2 r_{so}^5} R_{so} R_{so}^T$$

$$- \frac{c_s \tau^2}{r_{so}^4} L_o R_{so}^T + \frac{3\mu_p \tau^2}{2 r_p^5} (R_{so} - P)(R_{so} - P)^T \quad , \tag{64}$$

$$\frac{\partial R_s(t_i)}{\partial \dot{R}_s(t_{i-1})} = \tau I \quad , \tag{65}$$

$$\frac{\partial R_s(t_i)}{\partial W_o} = \frac{c\alpha_{20}}{W_o} T_o - \frac{c}{\dot{W}_o} (\alpha_{19} + \alpha_{20}) \dot{T}_o \quad , \tag{66}$$

$$\frac{\partial R_s(t_i)}{\partial \dot{W}_o} = - \frac{W_o}{\dot{W}_o} \frac{\partial R_s(t_i)}{\partial W_o} \quad , \tag{67}$$

$$\frac{\partial R_s(t_i)}{\partial c} = \alpha_{19} T_o - \alpha_{21} \dot{T}_o \quad , \tag{68}$$

$$\frac{\partial R_s(t_i)}{\partial p} = c\, \alpha_{19} (- \alpha_9 \hat{i} + \alpha_7 \hat{j})$$

$$- c\alpha_{21} \left[(\alpha_{10} \dot{y} - \alpha_7 \dot{p}) \hat{i} - (\alpha_8 \dot{y} + \alpha_9 \dot{p}) \hat{j}\right] \quad , \tag{69}$$

$$\frac{\partial R_s(t_i)}{\partial y} = c\alpha_{19}\,(-\alpha_8\,\hat{i} - \alpha_{10}\,\hat{j} + \alpha_5\,\hat{k})$$

$$- c\alpha_{21}\left[\,(-\alpha_7\,\dot{y} + \alpha_{10}\,\dot{p})\,\hat{i} - (\alpha_9\,\dot{y} + \alpha_8\,\dot{p})\,\hat{j}\right.$$

$$\left. - \alpha_6\,\dot{y}\,\hat{k}\,\right] \quad , \tag{70}$$

$$\frac{\partial R_s(t_i)}{\partial \dot{p}} = - c\alpha_{21}\,(-\alpha_9\,\hat{i} + \alpha_7\,\hat{j}) \quad , \tag{71}$$

$$\frac{\partial R_s(t_i)}{\partial \dot{y}} = - c\alpha_{21}\,(-\alpha_8\,\hat{i} - \alpha_{10}\,\hat{j} + \alpha_5\,\hat{k}) \quad , \tag{72}$$

$$\frac{\partial R_s(t_i)}{\partial \mu_s} = - \frac{\tau^2}{2r_{so}^3}\,R_{so} \quad , \tag{73}$$

$$\frac{\partial R_s(t_i)}{\partial \mu_p} = - \frac{\tau^2}{2}\left[\frac{R_{so} - P}{r_p^3} + \frac{P}{\pi^3}\right] \quad , \tag{74}$$

$$\frac{\partial R_s(t_i)}{\partial P} = \frac{\mu_p \tau^2}{2}\left(\frac{1}{r_p^3} - \frac{1}{\pi^3}\right) I - \frac{3\mu_p \tau^2}{2r_p^5}\,(R_{so}-P)\,(R_{so}-P)^T$$

$$+ \frac{3\mu_p \tau^2}{2\pi^5}\,PP^T \quad , \tag{75}$$

$$\frac{\partial R_s(t_i)}{\partial c_s} = \frac{\tau^2}{2r_{so}^2} L_o \quad , \tag{76}$$

$$\frac{\partial \dot{R}_s(t_i)}{\partial R_s(t_{i-1})} = -\tau \left(\frac{\mu_s}{r_{so}^3} + \frac{\mu_p}{r_p^3} \right) I + \frac{3\mu_s \tau}{r_{so}^5} R_{so} R_{so}^T$$

$$- \frac{2c_s \tau}{r_{so}^4} L_o R_{so}^T + \frac{3\mu_p \tau}{r_p^5} (R_{so}-P) (R_{so}-P)^T \quad , \tag{77}$$

$$\frac{\partial \dot{R}_s(t_i)}{\partial \dot{R}_s(t_{i-1})} = I \quad , \tag{78}$$

$$\frac{\partial \dot{R}_s(t_i)}{\partial W_o} = \alpha_1 c \left(\frac{\tau}{W_o} T_o - \frac{\alpha_{19}}{\dot{W}_o} \dot{T}_o \right), \tag{79}$$

$$\frac{\partial \dot{R}_s(t_i)}{\partial \dot{W}_o} = -\frac{W_o}{\dot{W}_o} \frac{\partial \dot{R}_s(t_i)}{\partial W_o} \quad , \tag{80}$$

$$\frac{\partial \dot{R}_s(t_i)}{\partial c} = \alpha_{18} T_o - \alpha_{20} \dot{T}_o \quad , \tag{81}$$

$$\frac{\partial \dot{R}_s(t_i)}{\partial p} = c\alpha_{18} (-\alpha_9 \hat{i} + \alpha_7 \hat{j})$$

$$- c\alpha_{20} \left[(\alpha_{10} \dot{y} - \alpha_7 \dot{p}) \hat{i} - (\alpha_9 \dot{p} + \alpha_8 \dot{y}) \hat{j} \right] \quad , \tag{82}$$

$$\frac{\partial \dot{R}_s(t_i)}{\partial y} = c\,\alpha_{18}\,(-\alpha_8\,\hat{i} - \alpha_{10}\,\hat{j} + \alpha_5\,\hat{k})$$

$$- c\,\alpha_{20}\left[(-\alpha_7\,\dot{y} + \alpha_{10}\,\dot{p})\,\hat{i} - (\alpha_9\,\dot{y} + \alpha_8\,\dot{p})\,\hat{j} - \alpha_6\,\dot{y}\,\hat{k}\right] \quad , \tag{83}$$

$$\frac{\partial \dot{R}_s(t_i)}{\partial \dot{p}} = - c\,\alpha_{20}\,(-\alpha_9\,\hat{i} + \alpha_7\,\hat{j}) \quad , \tag{84}$$

$$\frac{\partial \dot{R}_s(t_i)}{\partial \dot{y}} = - c\,\alpha_{20}(-\alpha_8\,\hat{i} - \alpha_{10}\,\hat{j} + \alpha_5\,\hat{k}) \quad , \tag{85}$$

$$\frac{\partial \dot{R}_s(t_i)}{\partial \mu_s} = - \frac{\tau}{r_{so}^3}\,R_{so} \quad , \tag{86}$$

$$\frac{\partial \dot{R}_s(t_i)}{\partial \mu_p} = - \tau\left[\frac{R_{so}-P}{r_p^3} + \frac{P}{\pi^3}\right] \quad , \tag{87}$$

$$\frac{\partial \dot{R}_s(t_i)}{\partial P} = \mu_p\,\tau\left(\frac{1}{r_p^3} - \frac{1}{\pi^3}\right) I - \frac{3\mu_p\,\tau}{r_p^5}\,(R_{so}-P)\,(R_{so}-P)^T$$

$$+ \frac{3\mu_p\,\tau}{\pi^5}\,PP^T \quad , \tag{88}$$

$$\frac{\partial \dot{R}_s(t_i)}{\partial c_s} = \frac{\tau}{r_{so}^2}\,L_o \quad . \tag{89}$$

The partial derivatives appearing in the matrices M and N of Section 5 are given as

$$\left[\frac{\partial\dot{\rho}}{\partial R_s}\right]^T = \frac{1}{\rho}\left[\dot{R}_\rho - \frac{(R_\rho^T \dot{R}_\rho)}{\rho^2} R_\rho\right] \quad , \tag{90}$$

$$\left[\frac{\partial\dot{\rho}}{\partial \dot{R}_s}\right]^T = \frac{R_\rho}{\rho} \quad , \tag{91}$$

$$\frac{d\dot{\rho}}{dt} = \frac{1}{\rho}\left[\dot{R}_\rho^T \dot{R}_\rho + R_\rho^T \ddot{R}_\rho - \frac{1}{\rho^2}\left(R_\rho^T \dot{R}_\rho\right)^2\right] \quad , \tag{92}$$

where

$$\rho = |R_\rho| ; \quad R_\rho = R_s - P_E - R_{st} ; \quad \dot{R}_\rho = \dot{R}_s - \dot{P}_E - \dot{R}_{st} ;$$

$$\ddot{R}_\rho = \ddot{R}_s - \ddot{P}_E - \ddot{R}_{st} ;$$

$$\dot{R}_{st} = \Omega_E \times R_{st} = \begin{bmatrix} -|\Omega_E| y_{st} \\ |\Omega_E| x_{st} \\ 0 \end{bmatrix} \quad ; \tag{93}$$

$$\ddot{R}_s = -\mu_s \frac{R_s}{r_s^3} ; \quad \ddot{P}_E = -\frac{(\mu_s + \mu_E) P_E}{|P_E|^3} ;$$

$$\ddot{R}_{st} = \Omega_E \times (\Omega_E \times R_{st}) \quad ;$$

and where $|\Omega_E|$ is the earth rotation rate. Also,

$$\left[\frac{\partial\theta_s}{\partial R_s}\right]^T = \frac{1}{|P-R_s|}\left\{\frac{|P-R_s|i_s - \frac{(P-R_s)^T i_s}{|P-R_s|}(P-R_s)}{\{|P-R_s|^2 - [(P-R_s)^T i_s]^2\}^{\frac{1}{2}}}\right\}, \tag{94}$$

$$\frac{\partial\theta_s}{\partial P} = -\frac{\partial\theta_s}{\partial R_s} \quad , \tag{95}$$

$$\frac{d\theta_s}{dt} = \frac{\partial\theta_s}{\partial R_s}(\dot{R}_s - \dot{P}) \quad , \tag{96}$$

$$\left[\frac{\partial\psi_s}{\partial R_s}\right]^T = \frac{2\,r_{eq}}{(|P-R_s|^2 - r_{eq}^2)^{\frac{1}{2}}|P-R_s|^2}(P-R_s) \quad , \tag{97}$$

$$\frac{\partial\psi_s}{\partial P} = -\frac{\partial\psi_s}{\partial R_s} \quad , \tag{98}$$

$$\frac{d\psi_s}{dt} = \frac{\partial\psi_s}{\partial R_s}(\dot{R}_s - \dot{P}) \quad . \tag{99}$$

APPENDIX A

We wish to include station location errors in the range rate observations of Eq. (36), as uncertain observation parameters.

Now station location errors are usually given in earth-fixed (u, v, w) coordinates with u → Greenwich and w → north pole. From Eq. (34) it is seen that range rate depends on

$$R_{st} = \begin{bmatrix} x_{st} \\ y_{st} \\ z_{st} \end{bmatrix} , \qquad \text{(A-1)}$$

which are the inertial coordinates of the station. We thus need a transformation from (u, v, w) to (x_{st}, y_{st}, z_{st}). The transformation is a single rotation

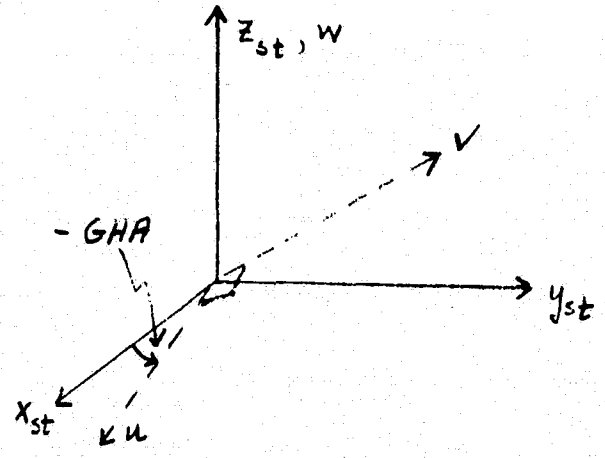

so that we have

$$\begin{bmatrix} x_{st} \\ y_{st} \\ z_{st} \end{bmatrix} = B \begin{bmatrix} u \\ v \\ w \end{bmatrix} \triangleq \begin{bmatrix} \cos GHA & \sin GHA & 0 \\ -\sin GHA & \cos GHA & 0 \\ 0 & 0 & 1 \end{bmatrix} \begin{bmatrix} u \\ v \\ w \end{bmatrix} . \qquad \text{(A-2)}$$

We easily compute

$$\left[\frac{\partial \dot{\rho}}{\partial R_{st}}\right]^T = \frac{1}{\rho}\left[\Omega_E \times R_\rho - \dot{R}_\rho\right] + \frac{\dot{\rho}}{\rho^2} R_\rho , \qquad \text{(A-3)}$$

and defining

$$\underset{A}{\overset{1x3}{}} \triangleq \left[\frac{\partial \dot{\rho}}{\partial R_{st}}\right]_{B}^{1x3\ \ 3x3} \quad , \qquad s \triangleq \begin{bmatrix} u \\ v \\ w \end{bmatrix} \quad , \tag{A-4}$$

the linearized range rate observation of Eq. (37) will now contain the additional term

$$\delta y_{\dot{\rho}} = \ldots + A\,\delta s \ . \tag{A-5}$$

Specific Modifications - In both modes 1 and 2

$$p^T \triangleq \left[\tau_{\dot{\rho}} \quad \delta P^T \quad \tau_a \quad \delta s^T\right] \ , \quad p \text{ is } 8x1 \ .$$

Mode 1

- U_p is 6x8: $U_p = \left[(U_p)_{old} \ \vdots \ 0_{6x3} \right]$

- $C_p(i|j)$ is 13x8

- W is 8x8 diagonal:

$$\text{diag } W = \left(\sigma^2_{\tau_{\dot{\rho}}}, \sigma^2_{P_1}, \sigma^2_{P_2}, \sigma^2_{P_3}, \sigma^2_{\tau_a}, \sigma^2_{\delta u}, \sigma^2_{\delta v}, \sigma^2_{\delta w}\right)$$

$\sigma_{\delta u}, \sigma_{\delta v}, \sigma_{\delta w}$ - additional input

- N is 1x8 (ground based tracking) :

$$N = \left[\frac{d\dot{\rho}}{dt} \ , \ 0, \ 0, \ 0, \ 0, \ A\right]$$

- N is 2x8 (on-board):

$$N = \left[\; (N)_{old} \;\vdots\; 0_{2x3} \; \right]$$

Mode 2

- U_p is 13x8: 13 x 5 U_p augmented with zeros

- $C_p(i|j)$ is 6x8

- W is 8x8 diagonal, as in Mode 1

- N is 1x8 (ground based tracking): same as in Mode 1

- N is 2x8 (on-board): same as in Mode 1

PART II

A S T E A

(ARBITRARY SPACE TRAJECTORY ERROR ANALYSIS)

COMPUTER PROGRAM UTILIZATION

1. Introduction

The effort under contract NAS5-11193 consisted of developing computer programs for the design, optimization and error analysis of low thrust interplanetary trajectories. Three computer programs were developed:

ASTEA - for the open-loop error analysis of arbitrary space trajectories (tailored for low thrust trajectories)

SWINGBY - for the optimization of low thrust swingby trajectories in the patched conic mode

ASTOP - for n-body, low thrust trajectory parameter optimization.

These programs are documented in the final reports prepared for the present contract by Analytical Mechanics Associates, Inc. Part II of this report describes the ASTEA computer program and contains its basic operating instructions.

2. The ASTEA Computer Program

ASTEA is an acronym for Arbitrary Space Trajectory Error Analysis. ASTEA was conceived to perform rapid error analysis for interplanetary missions involving electrically propelled spacecraft. The program is not restricted to low thrust propulsion, however, and is suitable for the error analysis of arbitrary space trajectories.

2.1 ASTEA General Program Description

The ASTEA (Arbitrary Space Trajectory Error Analysis) computer program performs an open-loop error analysis of arbitrary interplanetary trajectories. That is, it evaluates the performance of navigation systems with the space vehicle operating in an open-loop fashion: without guidance and control systems.

The theoretical analysis on which ASTEA is based is given in Part I. The fundamental characteristics of the computer program are

(1) Arbitrary trajectories, including optimal trajectories, can be handled. The trajectory is simply defined by a sequence of points.

(2) The use of an approximate, closed form model for partial derivatives (state transition matrix) required in the linearized error analysis obviates the time-consuming integration of variational equations.

(3) Arbitrary estimators (filters), specified by a gain sequence, can be analyzed. The Schmidt-Kalman filter with uncertain parameters is included as an option.

The model includes nineteen parameters associated with the dynamics (initial conditions or injection errors, propulsion system parameters, environmental parameters), and eight parameters associated with the navigation systems. Both radar tracking and on-board navigation are included.

All analytical details associated with the ASTEA program can be found in Part I. Here the computer program is described from the point of view of its utilization, including input and output, major subroutines, and program capabilities.

2.2 ASTEA Program Capabilities

The significant program capabilities are indicated here. Less significant capabilities are discussed in the description of program inputs. An understanding of these program capabilities and input instructions, together with an adequate comprehension of Part I, should enable the reader to run the ASTEA program successfully.

The ASTEA program will operate on any space trajectory, and is especially designed to handle trajectories involving continuously-thrusting spacecraft. In particular, ASTEA will perform an error analysis of optimum solar or nuclear electric missions with any number of coast periods. The reference trajectory is input as a sequence of points by either magnetic tape or cards. The analyst chooses a tracking history for the given trajectory and spacecraft, and this tracking history may involve up to thirty earth-based radar stations and an onboard optical tracking system. The tracking history is specified by setting a flag for each trajectory point which indicates if radar tracking, onboard optical tracking, neither, or both are to be simulated at that point.

The number of earth-based radar stations is specified at the start of program execution and may not vary along the trajectory. The radar stations simulate range-rate observations. The stations are located on a rotating, oblate earth, and, in general, only a subset of them are able to see the spacecraft at a given time. All stations have their viewing restricted according to a specified angle above the horizon. Spacecraft onboard tracking consists of observing the size of the target planet's disc (assumed circular), and of observing the angle between the target planet's center and a given star, defined by specifying its right ascension and declination.

The program has two basic operating modes, one in which only the spacecraft's position and velocity are estimated, and another in which, in addition to position and velocity, the significant parameters defining a continuously-thrusting spacecraft are estimated. These parameters are mass, mass flow rate, jet exhaust speed, thrust direction and its rate of change with time, where the thrust direction is defined by two angles, pitch and yaw. The initial variances of twenty-seven parameters, as cited in Part I, are specified. These are discussed in detail in the input instructions.

ASTEA is a multipurpose computer program, having sufficient versatility to allow an analyst to undertake several different types of investigations. This is best understood by noticing that the ASTEA operating philosophy consists of four basic components

1. Trajectory
2. Navigation System
3. Tracking History
4. Filter

This enables the analyst to perform the following four fundamental types of error analysis studies, and combinations thereof:

1. To identify favorable classes of trajectories, given a navigation system(s), tracking history, and filter,

2. To identify favorable navigation systems, given a trajectory, tracking history, and filter,

3. To identify favorable classes of tracking histories, given a trajectory, navigation system(s), and filter, and

4. To identify favorable classes of filters, given a trajectory, navigation system(s), and tracking history.

The fourth type of investigation is possible since the program permits the use of an arbitrary filter, as specified by an input filter gain sequence, or the use of the program's internal Schmidt-Kalman filter.

2.3 ASTEA Input and Output

INPUT

Card 1 (80A1) — Title

Card 2 (72I1) — NC(I) I = 1, 72 — Logic Control and Option Selection Flags

NC(1) = 1 Estimate position, velocity, and propulsion system parameters. (13x13) covariance matrix.
= 2 Estimate position and velocity only. (6x6) covariance matrix.

NC(2) = 1 Input Lagrange multipliers and their time-derivatives (for computing unit thrust vector).
= 2 Input thrust unit vector and its time-derivative.

NC(3) = 0 Input all vectors in earth-equatorial coordinates.
= 1 Input all vectors in ecliptic coordinates. (Program operates in the earth-equatorial system)

NC(4) = 0 Process earth radar tracking data first.
= 1 Process onboard optical tracking data first.

NC(5) = 0 Do not test covariance matrix positive-definiteness.
= 1 Test covariance matrix positive-definiteness after each propagation and after each observation, and print a single-line message.

NC(6) If $100\,NC(17) + 10\,NC(6) + NC(7) \neq 0$, then terminate the run after having processed that number of time-points. If = 0, program will attempt to process an unlimited number of time-points.

NC(7) [See NC(6).]

NC(8) = 0 Input jet exhaust speed c in meters/second and initial thrust acceleration a_o in meters/sec/sec.
= 1 Input c in AU/tau and a_o in AU/tau/tau. (Tau = 58.13244 days)

NC(9) Currently not used.

NC(10) = 0 Solar radiation pressure unit vector L_o is input (at each time point).

= 1 L_o is computed internally to be along the radius vector.

NC(11) = 0 Target planet ephemeris $(P_k, \dot{P}_k)$ is input at each time point.

= N, N=1, 9; Target planet ephemeris is computed internally, where N is the planet number, as follows:

N	Target Planet
1	Mercury
2	Venus
3	Earth
4	Mars
5	Jupiter
6	Saturn
7	Uranus
8	Neptune
9	Pluto

NC(12) Print flag.

= 0 Print only program inputs and standard deviations at last time-point.

= 1 Standard printout (standard deviations at each time-point after propagation and after processing observations.)

= 2 Longer print. Print matrices P, C_u, and C_p, and other parameters at each time-point.

= 9 Longest print [but not much longer than NC(12) = 2]. This causes print of a few more internal parameters (used for program checkout.)

Note: NC(12) = 2 or greater will cause excessive output if looking at many (say, 100) time-points.

NC(13) = 0 Flags Schmidt-Kalman filter (internal to program).

= 1 Requires that the filter gain sequence be input on cards (whether the trajectory and other parameters are input by cards or tape). If the trajectory is input by tape, then the filter gain cards are simply added to the end of the card deck (after cards 10.xx described below). If the trajectory is also input by cards,

then the filter gain cards must follow the trajectory cards (described below) for each time-point. If a potential observation is not made due to an internally-computed criterion (e.g., vehicle below horizon), the program will still read the required filter gain cards and therefore they must be present. For each observation, there will be at least one card (6D10.0), and if and only if NC(1) = 1, there will be a second card (7D10.0), corresponding to the ascending elements of the filter gain sequence associated with that observation.

NC(14) Currently not used.

NC(15) NTAPE = 10NC(15) + NC(16)
If NTAPE is greater than zero, the program assumes that the trajectory parameters (at each time-point) are being read from a tape mounted on logical unit NTAPE. (e.g., the card reader is logical unit 5.) If NTAPE = 0, the trajectory is read in by cards (described below). The tape format is described following these input instructions.

NC(16) [See NC(15).]

NC(17) [See NC(6).]

NC(18) = N, where N = 1, 2, 3, ..., 8, 9. If = 0, set equal to 1 internally. Whether inputting trajectory data by cards or tape, only every N^{th} time-point will be considered to exist, and all others (except endpoints and thrust switching points) will be totally ignored, as though they do not exist. This flag is used to ignore points when, for example, a given trajectory tape has an undesirable abundance of points.

NC(19)-NC(71) Currently not used.

NC(72) Unit 11 (RITS) print flag. Used for checkout purposes. Set equal to zero normally; set equal to 9 if RITS output (covariance matrix) is desired on unit 11 (Job language control card //GO.FT11F001 DD DSNAME= SYSOUT=R, DCB=(RECFM=FB, LRECL=80, BLKSIZE= 640) must be present when NC(72) ≠0.) If NC(12)=1, NC(72) is set equal to zero internally.

Card 3 (5I5, F5.2)	YEAR, MONTH, DAY, HOUR, MINUTE, and SECOND (respectively) corresponding to the first trajectory point. These are used for initiating the orientation of the earth for tracking the spacecraft by radar, and also for computing the base time for the internal analytic ephemeris routine, whenever such is desired [NC (11) $\neq 0$] for generating the target planet ephemeris. YEAR is the "launch" year (I5), e.g., 1977. By "launch" is meant the first trajectory point. MONTH is the month of the launch year (I5), e.g., August = 8. DAY is the day of launch within the launch month (I5), e.g., seventh day = 7. HOUR is the hour from midnight (GMT) of the launch day (I5), taking on values 0 through 23. MINUTE is the minute of launch (I5), taking on values 0 through 59. SECOND is the second of launch (F5.2), taking on values (0.) through (59.).
Card 4.00 (I10)	The number of radar stations to be used when tracking the spacecraft from the earth. This card must be followed by exactly (2 x number of radar stations) cards, where information pertaining to each radar station is input on two cards (such as in cards 4.01 and 4.02 described below). Zero (radar stations) is an admissible number, in which case cards 4.01 through 4.60 are absent. A maximum of 30 radar stations is admissible.
Card 4.01 (4A6)	Title describing the radar station. Used for printout purposes only.
Card 4.02 (7D10.0)	Position of radar station. The first three numbers are the longitude (degrees, minutes, seconds), the second three numbers are the latitude (degrees, minutes, seconds), and the seventh number is the altitude above an oblate earth, in feet.
Card 4.03 (4A6)	Title of radar station # 2.
Card 4.04 (7D10.0)	Position of radar station # 2.

.

.

.

Card 4.N(N-1) Title of last radar station

(4A6)

Card 4.NN Position of last radar station.

(7D10.0)

NOTE: There must be exactly (2 x number on card 4.00) cards pertaining to radar stations following card 4.00.

Card 5

(4D15.0)

HORANG, EMUP, C, AZERO, where

HORANG = the angle above the horizon at which the spacecraft becomes visible to each radar tracking station (degrees). This angle is the same for all stations.

EMUP = the target planet's gravity parameter, in AU^3/tau^2 (that is, relative to a solar gravity parameter of unity. For example, Venus's gravity parameter is about 0.2447E-5).

C = Spacecraft jet exhaust speed [meters/second if NC(8) = 0, AU/tau if NC(8) = 1].

AZERO = Spacecraft initial thrust acceleration [meters/sec/sec if NC(8) = 0, AU/tau/tau if NC(8) = 1].

Card 6

(4D15.0,11xI1)

WINIT, REQ, RAS, DEC, IALL, where

WINIT= Spacecraft initial mass (kilograms).

REQ= Target planet equatorial radius (kilometers).

RAS = Right ascension of star to be observed by the onboard tracking system (degrees).

DEC = Declination of star to be observed by the onboard tracking system (degrees).

IALL This applies only when the trajectory is read in by tape.

= 0 Read tape records indefinitely [unless terminated by NC(6), NC(7), and NC(17)].

= 1 Terminate reading of tape and program execution after reading (and processing) the final trajectory point (record) on the tape, regardless of the values of NC(6), NC(7), and NC(17).

Card 7

(8D8.0)

SIGMA (I), I=1,8. These are the initial error variances, or squares of the standard deviations. Vectors are with respect to the standard earth equatorial coordinate system (x-axis toward vernal equinox).

Notation: $\sigma(\tilde{x})$ is the error standard deviation of any parameter x; $\tilde{x} = x - \hat{x}$, where $\hat{x}$ is the best estimate.

SIGMA(1) = $\sigma^2(\tilde{x}_o)$ in $(AU)^2$.
SIGMA(2) = $\sigma^2(\tilde{y}_o)$ in $(AU)^2$.
SIGMA(3) = $\sigma^2(\tilde{z}_o)$ in $(AU)^2$.
} square of injection errors in position.

SIGMA(4) = $\sigma^2(\dot{\tilde{x}}_o)$ in $(AU/tau)^2$.
SIGMA(5) = $\sigma^2(\dot{\tilde{y}}_o)$ in $(AU/tau)^2$.
SIGMA(6) = $\sigma^2(\dot{\tilde{z}}_o)$ in $(AU/tau)^2$.
} square of injection errors in velocity.

(Tau = time to travel one radian in a circle of unit radius. One tau equals approximately 58 days.)

SIGMA(7) = $\sigma^2(\tilde{w}_o)$ in $(pounds)^2$. Spacecraft weight.

(One pound equals 0.4535924 kilograms.)

SIGMA(8) = $\sigma^2(\dot{\tilde{w}}_o)$ in $(pounds/tau)^2$. Spacecraft weight flow rate.

Card 8

(8D8.0)

SIGMA(I), I = 9, 16.

SIGMA(9) = $\sigma^2(\tilde{c})$ in $(AU/tau)^2$. Spacecraft jet exhaust speed.

SIGMA(10) = $\sigma^2(\tilde{p})$ in $(radians)^2$.
SIGMA(11) = $\sigma^2(\tilde{y})$ in $(radians)^2$.
} Pitch and yaw thrust angles.

SIGMA(12) = $\sigma^2(\dot{\tilde{p}})$ in $(radians/tau)^2$.
SIGMA(13) = $\sigma^2(\dot{\tilde{y}})$ in $(radians/tau)^2$.
} Pitch and yaw rates.

SIGMA(14) = $\sigma^2(\tilde{\mu}_s)$ in $(AU^3/tau^2)^2$. Gravitational constant of the sun (μ_s equals unity in these units).

SIGMA(15) = $\sigma^2(\tilde{\mu}_p)$ in $(AU^3/tau^2)^2$. Target planet gravitational constant = μ_p.

Card 9.1

(8D8.0)

SIGMA(I), I = 17, 24

SIGMA(16) = $\sigma^2(\tilde{P}_1)$ in $(AU)^2$.
SIGMA(17) = $\sigma^2(\tilde{P}_2)$ in $(AU)^2$.
SIGMA(18) = $\sigma^2(\tilde{P}_3)$ in $(AU)^2$.
} (P_1, P_2, P_3) is the target planet's position.

SIGMA(19) = $\sigma^2(\tilde{c}_s)$ in $(AU^3/tau^2)^2$. c_s is the coefficient of solar pressure.

SIGMA(20) = $\sigma^2(\tilde{\tau}_{\dot{\rho}})$ in $(tau)^2$. $\tau_{\dot{\rho}}$ is the radar timing error.

SIGMA(21) = $\sigma^2(\tilde{\tau}_a)$ in $(tau)^2$. τ_a is the timing error of the onboard tracking system.

SIGMA(22) = $\sigma^2(v_{\dot{\rho}})$ in $(AU/tau)^2$. Radar noise.

SIGMA(23) = $\sigma^2(v_{\theta_s})$ in $(radians)^2$. Star-sighting noise.

SIGMA(24) = $\sigma^2(v_{\psi_s})$ in $(radians)^2$. Target planet disc-sighting noise.

Card 9.2 (3D8.0)

SIGMA(I), I = 25, 27 Pertains to <u>all</u> radar station locations.

SIGMA(25) = $\sigma^2(\tilde{u})$, SIGMA(26) = $\sigma^2(\tilde{v})$, SIGMA(27)=$\sigma^2(\tilde{w})$, all in $(AU)^2$

Card 10.01 (72I1)

NPICK(I), I = 1, 72

Card 10.02 (72I1)

NPICK(I), I = 73, 144

Observation seclection flags.

.
.
.

Card 10.28 (72I1)

NPICK(I), I = 1945, 2016

I corresponds to the I^{th} trajectory point [not counting points which are ignored due to NC(18)].

NPICK(I) = 0 No observations at I^{th} trajectory point. [Propagation is always performed to each trajectory point which is considered to exist according to flag NC(18).]

= 1 Earth-based radar observations only.

= 2 Onboard optical observations only.

= 3 Both onboard and radar observations. The order of observations is controlled by the flag NC(4).

NPICK(1) is never used by the program. Observations are permitted beginning with the second trajectory point.

Notice that a maximum of 2016 trajectory points are currently allowed. If more than 2016 points are attempted,

the program will print a message and terminate execution at point 2016. This maximum number of trajectory points was imposed to avoid unnecessary program storage requirements (NPICK array), and may be easily extended.*

NPICK(72) = 9, NPICK(144) = 9, . . ., NPICK (2016) = 9 will flag the end of the NPICK cards. Thus, a 9 in card column 72 of, for example, card 10.05 indicates that cards 10.06 through 10.28 are absent. This means that unnecessary cards need not be present, which is especially helpful when the data is stored as a RITS file.

*Addendum: Maximum number of points has been extended to 8065.

If the trajectory is input by tape, there are no more cards (unless the filter gain sequence is input). Otherwise, the trajectory cards follow here, and each trajectory point is represented by five cards as follows (For inputting the filter gain sequence, see below Card I.5):

Card I.1 (3D15.0, 25xI2)

TI, WI, PRATIO, IEND, ITHR, where

TI = the time since the start of the trajectory (days).

WI = the mass ratio, current mass over initial mass (unitless).

PRATIO = the power ratio, current power available over power available at one AU from the sun. For nuclear electric spacecraft, PRATIO = 1 always. (unitless).

IEND Flag which indicates last trajectory point.

= 0 not last trajectory point.

= 1 last trajectory point.

ITHR Flag which indicates thrusting or coasting.

= 1 Indicates thrusting (and thrust-on switching points).

= 0 Indicates coasting (and thrust-off switching points).

Card I.2 (6D12.0)

RI(I), I = 1, 2, 3; RDI(I), I = 1, 2, 3, where

RI = spacecraft position vector at current time-point (AU).

RDI = spacecraft velocity vector at current time-point (AU/tau).

Note: <u>All</u> vectors must be expressed in either ecliptic or earth-equatorial coordinates, and the input flag NC(3) must then have the appropriate value.

Card I.3 (4D15.0)

ELI(I), I = 1, 2, 3; CSI, where

ELI = solar radiation pressure unit vector [See input flag NC(10).]

CSI = solar radiation pressure coefficient c_s (AU^3/tau^2).

Card I.4 (6D12.0)

PI(I), I = 1, 2, 3; PDI(I), I=1, 2, 3, where

PI = target planet position vector at current time-point (AU).

PDI = target planet velocity vector at current time-point (AU/tau).

Card I.5 (6D12.0)

If NC(2) = 1,

ELAM(I), I = 1, 2, 3; ELAMD(I), I = 1, 2, 3, where

ELAM = Primer vector (Lagrange multipliers adjoint to spacecraft velocity), in any units. This is merely a vector which lies along the thrust vector.

ELAMD = time derivative of ELAM (any units/tau).

If NC(2) = 2,

TT(I), I = 1, 2, 3; TTD(I), I = 1, 2, 3, where

TT = unit vector in direction of thrust (unitless).

TTD = time derivative of TT (tau^{-1}).

Note: The basic purpose of Card I.5 is to specify the thrust direction and its rate of change. This is accomplished for optimal trajectories* by using the Lagrange multiplier vector. Non-optimal thrust direction, and its rate of change, can be specified by some other vector, in particular, unit vectors. Therefore, the program should operate correctly if NC(2) = 1 always.

If the filter gain sequence is not input [NC(13)=0], then there are no more cards. Otherwise [NC(13)=1], the filter gain sequence for <u>each potential observation</u> which is allowed, according to the value of flag NPICK(I) for the current time-point, must be present. There will be either one card or two cards per potential observation. See the description of the flag NC(13) for further details.

If the trajectory is input by tape, the tape logical unit is specified by flags NC(15) and NC(16). The contents of the tape are nothing more than the contents of Cards I described directly above, and the format of each tape record is (30A8), so that each record consists of 30 words, each of length 8 in the A-format. If the tape logical unit is specified by NTAPE [see input flag NC(15)], then each tape record is created according to the following FORTRAN statement:

*Unconstrained optimal trajectories.

```
      WRITE (NTAPE, 100) TI, WI, PRATIO, ATHR, (RI(I), I = 1,3),
     (RDI(I), I = 1,3), (ELI(I), I = 1,3), CSI, (PI(I), I = 1,3),
     (PDI(I), I = 1,3), (ELAM(I), I = 1,3), (ELAMD(I), I = 1,3),
     AEND, UNIDUM, UNIDUM, UNIDUM
100  FORMAT (30 A 8)
```

where the names and their units are given directly above in the description of Cards I. UNIDUM (universal dummy variable) represents unused words. The ASTEA program reads the tape exactly according to the above WRITE statement. The tape is assumed to have the Lagrange multipliers (ELAM, ELAMD) as specifying the thrust vector, so that NC(2) must = 1 when reading the tape. Finally, ATHR and AEND are real names for integer quantities. ATHR and AEND must be related to ITHR and IEND, respectively, by means of an EQUIVALENCE statement.

OUTPUT

At each time-point, the standard deviations (square roots of diagonal elements of the covariance matrix) of all of the estimated parameters [six if NC(1)=2, thirteen if NC(1)=1] are printed out

1. After the covariance and correlation matrices are propagated from the prior point to the current point,

2. After all of the earth radar observations have been processed and the matrices updated (provided that radar observations are requested), and

3. After the onboard optical observations (star sighting and planet-disc sighting) have been processed and the matrices updated (provided that onboard observations are requested).

Using the notation described under Card 7, the first six elements SIGMA(I, I) printed (on a single line) are

$\sigma(\tilde{x})$, $\sigma(\tilde{y})$, $\sigma(\tilde{z})$ — Standard deviation of spacecraft position (km).

20

$\sigma(\tilde{\dot{x}})$, $\sigma(\tilde{\dot{y}})$, $\sigma(\tilde{\dot{z}})$ — Standard deviation of spacecraft velocity (meters/sec).

If estimating thirteen parameters [NC(1)=1], then a second line is printed:

$\sigma(\tilde{w})$ Standard deviation of spacecraft mass (kg).

$\sigma(\tilde{\dot{w}})$ Standard deviation of spacecraft mass flow rate (kg/day).

$\sigma(\tilde{c})$ Standard deviation of spacecraft jet exhaust speed (meters/sec).

$\sigma(\tilde{p})$ Standard deviation of thrust pitch angle (degrees).

$\sigma(\tilde{y})$ Standard deviation of thrust yaw angle (degrees).

$\sigma(\tilde{\dot{p}})$ Standard deviation of thrust pitch rate (degrees/day).

$\sigma(\tilde{\dot{y}})$ Standard deviation of thrust yaw rate (degrees/day).

A so-called "station see vector" is printed whenever earth radar observations are requested. This sequence of digits (0's and 1's) is ordered the same as the radar data is input to the program, and indicates whether (1) or not (0) a radar station was able to see the spacecraft at the given time.

When onboard optical tracking is requested at a given time-point, the two observation angles (target planet total disc and target-to-star angles) are printed in degrees.

All thrust switching points are clearly indicated.

The program inputs are described by the first three pages of output. The first page displays the date of launch (first trajectory point) and information pertaining to the earth-based radar tracking network. The other two pages display the input title, the flags NC(I), I=1,72, the initial variances, and other information describing the spacecraft, target planet, and observation specifications.

The above describes the ASTEA program's standard printout [NC(12)=1]. See the description of the input flag NC(12) for further details.

The following is a complete job input sequence (control cards and data) for running the trajectory error analysis program (ASTEA) on the IBM 360/91 at NASA Goddard. The trajectory is input on a 9-track tape as specified by the card / / GO. FT17..... (logical unit 17). Logical unit 11 is RITS output. The ASTEA program is procured by the name M7FIMERR from disk storage.

```
//YOUR JOB CARD
// EXEC LINKGO,REGION.GO=340K
//LINK.SYSLIN DD *
 INCLUDE LOADLIB(M7FIMERR)
 ENTRY MAIN
//GO.FT11F001 DD SYSOUT=R,DCB=(RECFM=FB,LRECL=80,BLKSIZE=640)
//GO.FT17F001 DD UNIT=2400-9,VOLUME=SER=TD5333,LABEL=(1,BLP),                X
//               DISP=(OLD,PASS),DCB=(RECFM=FB,BLKSIZE=1440,DEN=2)
//GO.DATA5 DD *
 SEP 8/24/77 650 DAY  EARTH TO JUPITER 2X38 ORBITER  T III X(1205)/C
1110000000100100170 1
 1977     8    24     0     0  0.0
          8          NO. STATIONS
 ALASKA
      212.        29.     5.7940        64.        58.    30.5720       900.0
 CARVON
      113.        42.    55.020        -24.        54.     14.860       124.
 FTHYRS
      278.         8.     3.8870        26.        32.    53.5160        12.
 JOBURG
       27.        42.    27.9310       -25.        52.    58.8620      4090.
 MADGAR
       47.        18.     0.4610       -19.         0.    27.0970      4518.
 ROSMAN
      277.         7.    41.230         35.        12.     0.710       2883.
 SNTAGO
      289.        19.    51.2830       -33.         8.    58.1060      2280.
 WNKFLD
      359.        18.    14.6150        51.        26.    44.1220       215.
10.              .954707726   -3 2.171269625 +4 1.784810838 -4
1.78533909   +369380.            100.25          -16.6                      1
4.468-194.468-194.468-191.127-091.127-091.127-091.549-011.094-00
4.783-041.218-031.218-035.929+045.929+041.000-109.115-134.468-11
4.468-114.468-112.116-133.964-183.964-183.538-159.402-119.402-11
0.       0.       0.
01111111111111111111111111111111111111111111111111111111111111111111
11111111111111111110101010101010101010101010101010101010101010101010
10101010101010101010101010101010101010101010101010101010101010101010
10101010101010101010101010101010101010101010101010101010101010101010
10101010101010101010101010101010101010101010101010101010101010101010
10101010101010101010101010101010101010101010101010101010101010101010
10101010101010101010101010101010101010101010101010101010101010101010
10101010101010101010101010101010101010101010101010101010101010101010
10101010101010101010101010100000000000000000000000000000000000000000
00000000000222222222222222222222222222222222222222222222000000000009
```

2.4 ASTEA Brief Subroutine Descriptions

Identification	Purpose
MAIN	Program master control. Reads cards 1 through 10.XX. Computes transition matrices and propagates error matrices in time.
APEFEM(TT, IB, RP, VP, NK)	Analytic ephemeris routine. TT = seconds elapsed since 1950 (input). IB = planet number [see flag NC(11) in the description of inputs], (input). RP = planet position (AU), (output). VP = planet velocity (AU/century), (output). NK = 1 compute both RP and VP, (input). = 0 compute only RP.
CROSS(A, B, C)	Computes cross product C = A x B for 3-vectors.
DCROUT	Called by POSDEF. This is also a matrix inversion routine.
INPUT	Trajectory input routine. Reads cards I.1 through I.5 or reads trajectory tape. Converts trajectory inputs to program internal units and earth-equatorial coordinates. Tests for thrust switching points. Computes unit vectors $\hat{i}$, $\hat{j}$, and $\hat{k}$. Terminates program execution.
MATMP(A, B, C, IL, IJ, IK, IND)	Matrix multiplication routine. A(IL, IJ), B(IJ, IK), C(IL, IK). IND = 1 $C = AB$ IND = 2 $C = AB^T$ IND = 3 $C = A^TB$ IND = 4 $C = A^TB^T$
NAVIG	Simulates and processes (filters) earth-based range-rate radar observations of spacecraft. Updates covariance matrices.
NAVIG2	Simulates and processes (filters) onboard optical tracking observations. Updates covariance matrices.

POSDEF(AA, IND, IXX, N, AAA, RR)	Tests positive definiteness of AA(N, N). IND is not used. IXX is an input identification number. AAA and RR are working arrays. This routine prints a message each time it is called.
PRINT(IPRINT)	Produces standard program printout [NC(12)=1]. IPRINT = 1 Prints results after propagation. = 2 Prints results after radar tracking. = 3 Prints results after onboard tracking.
PSICO(TT)	Called by RADAR. Produces orientation angle of earth at time TT.
RADAR(TTX, RADX, RADDX, IND, IREFNO)	Computes radar station radius vectors RADX in AU and their time derivatives. RADDX in AU/hour at time TTX, input in hours elapsed since the start of the trajectory. IREFNO=3 always, to select the earth. IND=1 reads in the radar data and computes the base time (time at start of trajectory). This occurs only once, at the beginning of program execution. IND=2 computes the positions and velocities of all the radar stations at the given time in earth equatorial coordinates. Also computes the position PE and velocity PDE of the earth (See APEFEM).
REDUCE(A1, A2)	Reduces A1 to modulo 2π and calls it A2.
ROTATE(X)	Transforms a vector X from ecliptic to earth equatorial coordinates.
SETUP	This routine initializes the covariance matrix and other matrices and prints them.
START(ISTART)	This routine zeros-out common blocks and initializes conversion constants and physical constants. Called once at start of execution only. ISTART is a dummy variable (not used). This routine is equivalent to BLOCK DATA except it will run on any machine which accepts standard FORTRAN.

UPELM	Called from APEFEM. Used to express APEFEM parameters as polynomial functions of time.
XAXT(M, N, X, A, XAX)	Computes XAX^T given X(M, N) and A(N, N).

2.5 ASTEA Machine Requirements.

ASTEA's core requirements on the NASA Goddard IBM 360/91 computer are 230B0 hexadecimal locations. The program is double precision FORTRAN IV, as specified by the nonstandard-FORTRAN statement IMPLICIT REAL*8 (A-H, O-Z) which appears at the beginning of each subroutine. Except for this method of double-precisioning the program, ASTEA consists of USA standard FORTRAN.

The CPU time (IBM 360/91) for the demonstration case given in this report was 132 seconds, and the I/O time was 32 seconds. The expected errors of thirteen parameters were estimated for 702 trajectory points, input to ASTEA by tape.

For peripheral equipment, ASTEA uses the standard UNIT 6 for printed output, and UNIT 5 for input by the card reader. In addition to these, the program uses UNIT 11 for output onto the NASA Goddard Remote Input Terminal System (RITS), which was used during checkout, and which can be ignored by setting the input flag NC(72) = 0. The use of RITS is not recommended during ASTEA runs, due to the slow printing capability of the RITS typewriter terminal. When a trajectory is input to ASTEA by magnetic tape, a tape unit specification is required. An example of the necessary job control cards for both RITS and for using a trajectory tape is given by the complete job input sequence which is displayed following the description of program output. The particular Jupiter trajectory tape used for this report's demonstration case was a fixed-blocked 800 bpi 9-track tape, as indicated by the displayed control cards. The tape was mounted on UNIT 17, as indicated by //GO.FT17 ..... However, any tape unit may be used, as specified by the two input flags NC(15) and NC(16). Moreover, any type of tape may be used as an ASTEA trajectory input tape, provided that the job control card is consistent with that tape, and provided that the tape's contents are consistent with the FORMAT statement given at the end of the description of program inputs.

2.6 ASTEA Numerical Results

The ASTEA program has been successfully applied to a 650-day optimum solar electric propulsion Jupiter orbiter mission with launch date 24 August 1977 and using a Titan III X(1205)/Centaur launch vehicle. The constant jet exhaust speed was 21712 meters/second and the initial thrust acceleration was 1.7848×10^{-4} meters/sec^2, corresponding to an initial power of 6.45 kw. The injection hyperbolic excess speed was 8105 meters/second, corresponding to an initial spacecraft mass of 1785 kg. The hyperbolic excess speed at Jupiter was 8550 meters/second, and a chemical retro stage inserted the spacecraft and a 550 kg scientific payload into a 2×38 (Jupiter radii) capture orbit. The optimum trajectory was a Mode A type of trajectory (having a heliocentric travel angle of 164 degrees), as defined in [3], and contained one interior coast period commencing at 337 days and terminating at 543 days.

The Jupiter trajectory contained 702 points and was fed into ASTEA by tape. The tape was generated by the optimum low thrust trajectory program HILTOP, which has recently been documented in [4]. Since HILTOP employs the generalized universal anomaly as the independent variable of integration, each integration step does not correspond to a fixed time increment. The tape was generated by writing the necessary quantities onto it at each integration step, and this corresponded to time increments of about 0.25 days near Earth and 2.8 days near Jupiter. Furthermore, HILTOP is a two-body program, designed primarily for performance analysis studies, and therefore the trajectory did not include the gravitational pull of Jupiter on the spacecraft. Nevertheless, the results quoted below are believed to be representative of the uncertainties which will accrue during a heliocentric flight from the Earth to Jupiter by a solar electric spacecraft for the tracking history employed.

The tracking history used for this demonstration case consisted of simulating earth-based radar observations prior to the coast period, no observations during the coast period, and optical tracking of Jupiter's disc and the angle between Jupiter and the star Sirius (right ascension 100.25 degrees, declination - 16.6 degrees) by the onboard system after the coast period. The explicit tracking history is given by the ten NPICK cards (the last ten cards) of the complete job input sequence which is displayed following the description of program output. The job input sequence given there is exactly the one used to generate this demonstration case. The earth-based radar tracking consisted of eight radar stations, each having a horizon visibility angle of ten degrees. The program's internal Schmidt-Kalman filter was used.

All thirteen parameters [NC (1) = 1] mentioned in Section 2.2 were estimated and improved by the tracking. The input initial variances corresponded to the following standard deviations:

$\sigma(\tilde{x}_o)$, $\sigma(\tilde{y}_o)$, $\sigma(\tilde{z}_o)$ — 100 meters.

$\sigma(\tilde{\dot{x}}_o)$, $\sigma(\tilde{\dot{y}}_o)$, $\sigma(\tilde{\dot{z}}_o)$ — 1.0 meters/second.

$\sigma(\tilde{w}_o)$ — 0.01% of w_o.

$\sigma(\tilde{\dot{w}}_o)$ — 2% of trajectory-average $\dot{w}$.

$\sigma(\tilde{c})$ — 3% of c.

$\sigma(\tilde{p})$ — 2 degrees

$\sigma(\tilde{y})$ — 2 degrees

$\sigma(\tilde{\dot{p}})$ — 10 degrees/hour

$\sigma(\tilde{\dot{y}})$ — 10 degrees/hour

$\sigma(\tilde{\mu}_s)$ — 10^{-5} AU^3/tau^2.

$\sigma(\tilde{\mu}_p)$ — 0.1% of μ_p in AU^3/tau^2.

$\sigma(\tilde{P}_1)$, $\sigma(\tilde{P}_2)$, $\sigma(\tilde{P}_3)$ — 1000 kilometers.

$\sigma(\tilde{c}_s)$	10% of c_s in AU^3/tau^2.	$\sigma(\tilde{u})$	
$\sigma(\tilde{\tau}_{\dot{\rho}})$	10 milliseconds.	$\sigma(\tilde{v})$	0
$\sigma(\tilde{\tau}_a)$	10 milliseconds.	$\sigma(\tilde{w})$	
$\sigma(V_{\dot{\rho}})$	10^{-6} earth radii/hour.		
$\sigma(V_{\theta_s})$	2 seconds of arc.		
$\sigma(V_{\psi_s})$	2 seconds of arc.		

The state estimation errors along the trajectory are summarized in Table 1. Results are not quoted for the final trajectory point (650.000 days) because that point lies inside the planet Jupiter, as this is how HILTOP generates trajectories. The observations by the onboard system during Jupiter encounter were made at each available trajectory point, i.e., about every 2.8 days. It is felt that a tracking history employing more frequent observations during Jupiter encounter would yield a more favorable state estimation. However, ASTEA is currently limited to simulating observations only at the available trajectory points. At the last trajectory point before Jupiter impact (649.147 days), the angle between Jupiter and Sirius was 39.13 degrees (as seen by the spacecraft), and the angle subtended by Jupiter's disc was 12.73 degrees.

The state estimation errors given at time 600.555 days in Table 1, for the assumptions made for this demonstration case, may be considered as representative of the uncertainty in the estimation of a solar-electric spacecraft's state as it approaches Jupiter along the encounter asymptote. It is interesting to consider the influence which position estimation errors can have on the final capture orbit about Jupiter. The 1σ errors in the position only, 50 days before Jupiter arrival, propagate into capture orbit (nominal 2 x 38) errors which may result in the following capture orbits:

1σ smallest - periapse orbit	(1.98 x 37.71)	Jupiter radii
nominal orbit	(2.00 x 38.00)	
1σ largest - periapse orbit	(2.02 x 38.29)	

Of course, onboard tracking during Jupiter encounter will improve the estimate of the capture orbit to yield a better estimate than that implied above. The above is nothing more than a simple propagation of the 1σ position errors only, to obtain a crude idea of how bad the capture orbit might be if there is no tracking during the last 50 days. The calculation assumes that the spacecraft approaches Jupiter along the nominal

asymptote (except for the position uncertainty) with the nominal speed, and the chemical retro stage performs the nominal velocity increment to insert the 550 kg payload into a Jupiter capture orbit. The computation of the errors in the capture orbit do not include error sources such as velocity errors, errors in Jupiter mass and ephemeris, and errors in spacecraft parameters.

TABLE 1

STATE ESTIMATION ERRORS FOR 650-DAY JUPITER MISSION

(Demonstration Case)

Time from launch (days)	$\sigma(\tilde{x})$ (km)	$\sigma(\tilde{y})$ (km)	$\sigma(\tilde{z})$ (km)	$\sigma(\dot{\tilde{x}})$ (m/sec)	$\sigma(\dot{\tilde{y}})$ (m/sec)	$\sigma(\dot{\tilde{z}})$ (m/sec)
0.000	0.1000	0.1000	0.1000	0.99990	0.99990	0.99990
100.265	111.7796	123.5208	240.2157	0.05129	0.05353	0.10202
200.356	347.5437	271.3726	592.1656	0.05843	0.04458	0.09766
299.988	671.1526	424.0673	886.4852	0.05238	0.0660	0.09343
336.617 Begin Coast	689.9767	544.8630	1052.5563	0.04218	0.07212	0.09776
542.887 End Coast	1391.9283	1598.5064	1186.3643	0.05174	0.12976	0.06105
600.555	1516.3363	2362.0235	1292.6126	0.05603	0.33388	0.14270
649.147	1048.8546	987.7692	921.2665	10.17885	2.90675	1.03005

3. Conclusions and Recommendations

The ASTEA computer program has been successfully demonstrated on a 650-day optimum solar electric propulsion Jupiter orbiter mission (see Section 2.6). The program is operational and ready for use.

It is believed that certain additions and modifications to the program would enhance its usefulness. Recommendations for these additions and modifications follow:

(1) Incorporate errors in the time of engine ignition and cutoff.

(2) Provide for re-initialization of propulsion system error statistics at re-ignition.

(3) Provide for the re-orientation of the attitude reference.

(4) Include a catalog of stars for on-board navigation.

(5) Incorporate capability of observing the disc angle of the departure and swingby planets.

(6) Incorporate logic and appropriate interpolation to allow for navigation at time-points where no trajectory information is available by input. Also, incorporate logic for skipping points at which no navigation is desired.

REFERENCES

[1] S. Pines, "The Propagation of Position and Velocity Uncertainties Through Thrust Maneuvers," Paper presented at the AIAA/NASA-MSC Astrodynamics Conference, Houston, Texas, December 12-13, 1967.

[2] A. H. Jazwinski, Stochastic Processes and Filtering Theory, Academic Press, New York, 1969.

[3] J. L. Horsewood and F. I. Mann, "Optimum Solar Electric Interplanetary Trajectory and Performance Data", NASA CR-1524, April 1970.

[4] P. F. Flanagan and J. L. Horsewood, "HILTOP: Heliocentric Interplanetary Low Thrust Trajectory Optimization Program," Analytical Mechanics Associates, Inc., Report No. 70-46, December 1970.